

DG APPROACH TO LARGE BENDING PLATE DEFORMATIONS WITH ISOMETRY CONSTRAINT

ANDREA BONITO¹, RICARDO H. NOCHETTO², AND DIMITRIOS NTOGKAS³

ABSTRACT. We propose a new discontinuous Galerkin (dG) method for a geometrically nonlinear Kirchhoff plate model for large isometric bending deformations. The minimization problem is nonconvex due to the isometry constraint. We present a practical discrete gradient flow that decreases the energy and computes discrete minimizers that satisfy a prescribed discrete isometry defect. We prove Γ -convergence of the discrete energies and discrete global minimizers. We document the flexibility and accuracy of the dG method with several numerical experiments.

1. INTRODUCTION

Large bending deformations of thin plates is a critical subject for many modern engineering applications due to the extensive use of plate actuators in a variety of systems like thermostats, nano-tubes, micro-robots and micro-capsules [9, 23, 26, 32, 33]. From the mathematical viewpoint, there is an increasing interest in the modeling and the numerical treatment of such plates. A rigorous analysis of large bending deformations of plates was conducted by Friesecke, James and Müller [22], who derived the geometrically non-linear Kirchhoff model from three dimensional hyperelasticity. Since then, there have been various other interesting models, such as the prestrained models derived in [10, 27]. Previous work on the numerical treatment of large bending deformations includes the single layer problem by Bartels [5], the bilayer problem by Bartels, Bonito and Nochetto [8] and the modeling and simulation of thermally actuated bilayer plates by Bartels, Bonito, Muliana and Nochetto [7]. In all three approaches the model involves minimizing an energy functional that is dominated by the Hessian of the deformation $y : \Omega \rightarrow \mathbb{R}^3$ of the mid-plane Ω of the plate. The minimization takes place under Dirichlet boundary conditions for y and ∇y and the isometry constraint

$$(1.1) \quad \nabla y^T \nabla y = I \quad \text{a.e. in } \Omega,$$

where I stands for the identity matrix in \mathbb{R}^2 . The authors employ Kirchhoff elements in order to impose the isometry constraint at the nodes of the triangulation and rely on an H^2 -gradient flow that allows them to construct solutions of decreasing discrete energy. In [5, 8] it is also proved that the discrete energy Γ -converges to the continuous one. Since for higher order problems a conforming approach would

¹ Partially supported by the NSF Grant DMS-1817691.

² Partially supported by the NSF Grants DMS-1411808 and DMS-1908267, the Institut Henri Poincaré (Paris) and the Hausdorff Institute (Bonn).

³ Partially supported by the NSF Grant DMS-1411808 and the 2016-2017 Patrick and Marguerite Sung Fellowship of the University of Maryland.

be very costly, the Kirchhoff elements offer a natural non-conforming space for the model that allows the imposition of (1.1) nodewise.

1.1. Our contribution. In this paper we focus on the single layer problem, in order to investigate the applicability of a more flexible approach that hinges on a non-conforming space of discontinuous functions and the use of interior penalty terms for the discrete energy, along with a Nitsche approach to enforce the boundary conditions in the limit. We start with the Dirichlet and forcing data

$$(1.2) \quad g \in [H^1(\Omega)]^3, \quad \Phi \in [H^1(\Omega)]^{3 \times 2}, \quad f \in [L^2(\Omega)]^3,$$

and the affine manifold of $[H^2(\Omega)]^3$

$$(1.3) \quad \mathbb{V}(g, \Phi) := \{v \in [H^2(\Omega)]^3 : v = g, \nabla v = \Phi \text{ on } \partial_D \Omega\},$$

where $\partial_D \Omega$ is an open set of the boundary $\partial \Omega$ so that $|\partial_D \Omega| \neq 0$. We wish to approximate a minimizer $y : \Omega \rightarrow \mathbb{R}^3$ of the continuous energy

$$(1.4) \quad E[y] = \frac{1}{2} \int_{\Omega} |D^2 y|^2 - \int_{\Omega} f y$$

in the nonconvex set of admissible functions

$$(1.5) \quad \mathbb{A} = \{y \in \mathbb{V}(g, \Phi) : (\nabla y)^T \nabla y = I \text{ a.e. in } \Omega\},$$

where $|\cdot|$ denotes the Frobenius norm. In order to avoid the costly use of a conforming finite element subspace of $[H^2(\Omega)]^3$, we use a space \mathbb{V}_h^k of discontinuous piecewise polynomials of degree $k \geq 2$. Associated with \mathbb{V}_h^k , we introduce a discrete energy E_h that approximates the energy E and accounts for the discontinuities of the functions $v_h \in \mathbb{V}_h^k$ and of their piecewise gradients $\nabla_h v_h$.

It is important to notice that the energy E in (1.4) is convex but the isometry constraint (1.1) is not. Therefore, we must approximate (1.1), and thus the admissible set \mathbb{A} in a way amenable to computation, as well as construct an algorithm able to find discrete minimizers. We define the discrete admissible set $\mathbb{A}_{h,\delta}^k$ to be the set of functions $v_h \in \mathbb{V}_h^k$ whose *discrete isometry defect* $D_h[v_h]$ satisfies

$$(1.6) \quad D_h[v_h] := \sum_{T \in \mathcal{T}_h} \left| \int_T (\nabla_h v_h)^T \nabla_h v_h - I \right| \leq \delta,$$

where $\delta = \delta(h) \rightarrow 0$ as $h \rightarrow 0$. We then search for $y_h \in \mathbb{A}_{h,\delta}^k$ that minimizes the discrete energy $E_h[y_h]$. To this end, we propose a discrete H^2 -gradient flow. We show that it gives rise to iterates $\{y_h^n\}_{n=1}^\infty$ with decreasing discrete energy $E_h[y_h^{n+1}] < E_h[y_h^n]$, whenever $y_h^{n+1} \neq y_h^n$, and guarantees the discrete isometry defect (1.6) for all $n \geq 1$ provided the initial guess $y_h^0 \in \mathbb{V}_h^k$ is an approximate isometry so that $D_h[y_h^0] \leq \tau$ and δ is proportional to $E_h[y_h^0]\tau$. Hereafter, τ is the fictitious time step in the discrete gradient flow and can be made arbitrarily small.

We also prove Γ -convergence of the discrete energy E_h to the continuous energy E and that global minimizers of E_h in $\mathbb{A}_{h,\delta}^k$ converge in $L^2(\Omega)$ to global minimizers of E in \mathbb{A} as $h \rightarrow 0$. A key ingredient for Γ -convergence is reconstruction of a suitable discrete Hessian $H_h[v_h]$ for discontinuous functions $v_h \in \mathbb{V}_{h,\delta}^k$. A similar approach is employed in [19] for second order problems and later in [30] for the p -biharmonic equation, where $p = 2$ leads to the same construction as ours.

Our approach is motivated by the flexibility of dG compared to Kirchhoff elements. First of all, Kirchhoff elements require polynomial degree $k = 3$ and suffer from a complicated implementation that involves a discrete gradient that maps the

gradient of the discrete deformation to another space. Since this is not implemented in standard finite element libraries, the above difficulty hinders the impact of the method in the engineering community. In contrast, the proposed dG approach works for $k \geq 2$, does not require such map (or more precisely, the map is the trivial elementwise differentiation) and its implementation is standard. Moreover, unlike the dG formulation, Kirchhoff elements are not amenable to adaptively refined partitions, at least in theory. It is worth mentioning as well that imposing Dirichlet boundary conditions weakly, instead of directly in the admissible set as in [8, 7], allows for more flexibility. In particular, this alleviates the constraints on the construction of the recovery sequence necessary for the Γ -convergence of E_h towards E ; see Section 5.3. Upon dropping the penalty term of jumps of ∇y_h across a prescribed curve, dG naturally accommodates configurations with edges, as is the case of origami. Lastly, imposing the isometry constraint numerically with Kirchhoff elements at each vertex seems to be very rigid at the expense of approximation accuracy. In contrast, our experiments with dG indicate that this approach is more accurate and adjusts better to the geometry of the problem; see Section 6.1.

1.2. Outline. We first construct our discrete energy functional E_h in Section 2, using as motivation the biharmonic problem. We also prove some key properties for functions $v_h \in \mathbb{V}_h^k$, including the coercivity of E_h with respect to an appropriate mesh-dependent energy norm. We introduce in Section 3 the discrete H^2 -gradient flow and show it is able to find discrete minimizers of E_h that satisfy the desired discrete isometry defect (1.6); this sets the stage for relation between δ, h and τ in (1.6). In Section 4 we define the discrete Hessian $H_h[y_h]$ and derive a bound in L^2 and its weak convergence in L^2 . This leads to the proof of Γ -convergence of the discrete energy E_h to the exact energy E , in Section 5, and then the convergence of global minimizers of E_h to global minimizers of E . In Section 6 we present experiments that corroborate numerically the excellent properties of our method and compare it with the Kirchhoff element approach. In Section 7 we provide some details for our implementation and justify the choice of a discontinuous versus a continuous space of functions \mathbb{V}_h^k . Lastly, we draw conclusions in Section 8.

2. DISCRETE ENERGY AND PROPERTIES OF dG

We start this section by providing intuition on the derivation of the discrete energy E_h , but without presenting all the details. We then introduce the discrete dG space \mathbb{V}_h^k along with an interpolation operator $\Pi_h : \prod_{T \in \mathcal{T}_h} H^1(T) \rightarrow \mathbb{V}_h^k \cap H^1(\Omega)$, and discuss its properties. We finally prove coercivity of E_h .

2.1. Continuous energy. Starting from a three-dimensional hyperelasticity model, dimension reduction as the thickness of the plate decreases to zero leads to the two-dimensional energy functional [5]

$$(2.1) \quad E[y] = \frac{1}{2} \int_{\Omega} |H|^2 - \int_{\Omega} f y,$$

up to a multiplicative constant for the first term. here $y \in \mathbb{A}$ is the isometric deformation of $\Omega \subset \mathbb{R}^2$ into \mathbb{R}^3 , $H = (h_{ij})_{i,j=1}^2 := (\partial_{ij} y \cdot \nu)_{i,j=1}^2$ is the second fundamental form of the deformed plate $y(\Omega)$ and $\nu := \partial_1 y \times \partial_2 y$ is its unit normal. The connection between (2.1) and (1.4) follows from the isometry property of y :

$$\partial_i y \cdot \partial_j y = \delta_{ij}, \quad i, j = 1, 2.$$

Differentiating with respect to x_1 and x_2 and using simple algebraic manipulations, these relations imply

$$\partial_k y \cdot \partial_{ij} y = 0 \implies \partial_{ij} y \parallel \nu = \partial_1 y \times \partial_2 y, \quad i, j, k = 1, 2.$$

This, combined with the definition $h_{ij} = \partial_{ij} y \cdot \nu$, leads in turn to

$$|h_{ij}|^2 = |\partial_{ij} y|^2$$

and justifies the energy (1.4). Similarly, using that

$$\partial_1 (\partial_{12} y \cdot \partial_2 y) = 0 \quad \text{and} \quad \partial_2 (\partial_{11} y \cdot \partial_2 y) = 0,$$

we obtain

$$|\partial_{12} y|^2 = \partial_{11} y \cdot \partial_{22} y.$$

Therefore, the isometry property yields the pointwise relations

$$(2.2) \quad |H|^2 = |D^2 y|^2 = |\Delta y|^2,$$

so that the expression (2.1) of $E[y]$ coincides with (1.4), namely

$$(2.3) \quad E[y] = \frac{1}{2} \int_{\Omega} |D^2 y|^2 - \int_{\Omega} f y.$$

The Euler-Lagrange equation for a minimizer $y \in \mathbb{V}(g, \Phi)$ of (2.3) reads

$$(2.4) \quad \int_{\Omega} D^2 y : D^2 v = \int_{\Omega} f v \quad \forall v \in \mathbb{V}(0, \mathbf{0}),$$

where $\mathbb{V}(g, \Phi)$ is defined in (1.3). The strong form of (2.4) is $\operatorname{div} \operatorname{div} D^2 y = f$ whereas the natural boundary conditions imposed on $\partial\Omega \setminus \partial_D \Omega$ are

$$(2.5) \quad \partial_{\mu} \nabla y = D^2 y \mu = 0, \quad \partial_{\mu} \Delta y = (\operatorname{div} D^2 y) \mu = 0.$$

Here μ denotes the outside pointing (co-)normal to Ω .

2.2. Discrete energy. We assume that Ω is a polygonal domain in \mathbb{R}^2 and consider a sequence of subdivisions $\{\mathcal{T}_h\}_{h>0}$ of Ω made of shape regular elements [18] (either triangles or quadrilaterals). We assume that these meshes are quasi-uniform and identify h with the maximal element size. From now on c and C are generic constants independent of h but possibly depending on the shape-regularity and quasi-uniformity constants of the sequence $\{\mathcal{T}_h\}_{h>0}$. Also, we use the notation $A \lesssim B$ to indicate $A \leq cB$, where c is a constant independent of h , A and B .

We denote by \mathbb{P}_k (resp. \mathbb{Q}_k) the space of polynomial functions of degree at most $k \geq 0$ (resp. at most k on each variable). Also, \hat{T} stands for the reference element, which is either the two dimensional simplex when the subdivision is made of triangles or the unit square in the case of quadrilaterals. The mapping between the reference element \hat{T} and any $T \in \mathcal{T}_h$ is denoted F_T . Notice that F_T is affine for triangles T and bi-linear for quadrilaterals T .

With each subdivision \mathcal{T}_h made of triangles, we associate the space of discontinuous piecewise polynomial functions

$$(2.6) \quad \mathbb{V}_h^k := \{v_h \in L^2(\Omega) : \forall T \in \mathcal{T}_h, \quad v_h|_T = \hat{v}_h \circ F_T^{-1} \text{ for some } \hat{v}_h \in \mathbb{P}_k\}.$$

Alternatively for subdivisions made of quadrilaterals, the space \mathbb{P}_k is replaced by \mathbb{Q}_k . We point out that in that case, $v_h|_T$ is not polynomial, which entails additional difficulties accounted for in the analysis below. In both cases, we require $k \geq 2$.

We denote by \mathcal{E}_h^0 the collection of edges of \mathcal{T}_h contained in Ω and by \mathcal{E}_h^b those contained $\partial_D \Omega$; hence $\mathcal{E}_h = \mathcal{E}_h^0 \cup \mathcal{E}_h^b$ is the set of active interelement boundaries. We

further denote by $\Gamma_h^0 := \cup\{e : e \in \mathcal{E}_h^0\}$ the interior skeleton, by $\Gamma_h^b := \cup\{e : e \in \mathcal{E}_h^b\}$ the boundary counterpart, and by $\Gamma_h := \Gamma_h^0 \cup \Gamma_h^b$ the full skeleton.

For $e \in \mathcal{E}_h^0$ we fix $\mu := \mu_e$ to be one of the two unit normals to e in Ω ; this choice is irrelevant for the discussion below. Given $v_h \in \mathbb{V}_h^k$, we denote its piecewise gradient by $\nabla_h v_h$ and their *jumps* across interior edges $e \in \mathcal{E}_h^0$ by

$$(2.7) \quad [v_h] := v_h^- - v_h^+, \quad [\nabla_h v_h] := \nabla_h v_h^- - \nabla_h v_h^+,$$

where $v_h^\pm(x) = \lim_{s \rightarrow 0} v_h(x \pm s \mu_e)$. In order to deal with Dirichlet boundary data (1.2), we define the discrete counterpart of $\mathbb{V}(g, \Phi)$ to be

$$(2.8) \quad \mathbb{V}_h^k(g, \Phi) := \{v_h \in [\mathbb{V}_h^k]^3 : [v_h]_e := v_h - g, [\nabla_h v_h]_e := \nabla_h v_h - \Phi \quad \forall e \in \mathcal{E}_h^b\};$$

we thus append a notion of jump on the Dirichlet boundary $\partial_D \Omega$ that corresponds to μ_e to be the outward pointing normal to e in Ω . Moreover, note that boundary jumps are $[v_h] := v_h$ and $[\nabla_h v_h] := \nabla_h v_h$ for all $v_h \in \mathbb{V}_h^k(0, \mathbf{0})$. The *average* of $v_h \in \mathbb{V}_h^k(g, \Phi)$ across an edge $e \in \mathcal{E}_h$ is given by

$$(2.9) \quad \{v_h\} := \begin{cases} \frac{1}{2}(v_h^+ + v_h^-) & e \in \mathcal{E}_h^0 \\ v_h^- & e \in \mathcal{E}_h^b \end{cases}, \quad \{\nabla_h v_h\} := \begin{cases} \frac{1}{2}(\nabla_h v_h^+ + \nabla_h v_h^-) & e \in \mathcal{E}_h^0 \\ \nabla_h v_h^- & e \in \mathcal{E}_h^b \end{cases}.$$

Before introducing the discrete energy E_h we derive the corresponding bilinear form $a_h(\cdot, \cdot)$ in the usual manner. We integrate by parts twice the strong equation $\operatorname{div} \operatorname{div} D^2 y = f$ over elements $T \in \mathcal{T}_h$ against a test function $v_h \in \mathbb{V}_h^k(0, \mathbf{0})$, collect the jumps on edges e and realize that $[\partial_\mu \nabla y] = 0$ and $[\partial_\mu \Delta y] = 0$ on all edges e (including those on $\partial \Omega \setminus \partial_D \Omega$ because of (2.5)), symmetrize the expression, and add penalty terms with parameters $\gamma_0, \gamma_1 > 0$. We point out that we are allowed to add the terms $\nabla y - \Phi$ and $y - g$ on Γ_h^0 during the symmetrization process because they vanish for $y \in \mathbb{V}(g, \Phi)$. Altogether, this gives the equation

$$(2.10) \quad \begin{aligned} a_h(y_h, v_h) &:= (D_h^2 y_h, D_h^2 v_h)_{L^2(\Omega)} \\ &\quad - (\{\partial_\mu \nabla_h y_h\}, [\nabla_h v_h])_{L^2(\Gamma_h)} - (\{\partial_\mu \nabla_h v_h\}, [\nabla_h y_h])_{L^2(\Gamma_h)} \\ &\quad + (\{\partial_\mu \Delta_h y_h\}, [v_h])_{L^2(\Gamma_h)} + (\{\partial_\mu \Delta_h v_h\}, [y_h])_{L^2(\Gamma_h)} \\ &\quad + \gamma_1 (h^{-1} [\nabla_h y_h], [\nabla_h v_h])_{L^2(\Gamma_h)} + \gamma_0 (h^{-3/2} [y_h], [v_h])_{L^2(\Gamma_h)} \\ &= (f, v_h)_{L^2(\Omega)}, \end{aligned}$$

for $y_h \in \mathbb{V}_h^k(g, \Phi)$ and $v_h \in \mathbb{V}_h^k(0, \mathbf{0})$. We note that the Dirichlet conditions on $\partial_D \Omega$ are enforced in the Nitsche's sense. Since a_h is symmetric by construction, we let

$$(2.11) \quad E_h[y_h] := \frac{1}{2} a_h(y_h, y_h) - (f, y_h)_{L^2(\Omega)},$$

and note that (2.10) is the first variation $\delta E_h[y_h; v_h]$ of $E_h[y_h]$ in the direction v_h .

In order for (2.11) to be meaningful with respect to the original minimization problem in (1.4)-(1.5), we define the *discrete admissible set* $\mathbb{A}_{h,\delta}^k$, a discrete analogue of \mathbb{A} in (1.5) that involves the discrete isometry defect D_h , to be

$$(2.12) \quad \mathbb{A}_{h,\delta}^k := \left\{ y_h \in \mathbb{V}_h^k(g, \Phi) : D_h[y_h] = \sum_{T \in \mathcal{T}_h} \left| \int_T (\nabla_h y_h)^T \nabla_h y_h - I \right| \leq \delta \right\},$$

with parameter $\delta = \delta(h) \rightarrow 0$ as $h \rightarrow 0$. We will see in Section 3 that the discrete gradient flow used to construct discrete solutions yields $\delta \leq Ch$, where C is proportional to $E_h[y_h^0]$ and other geometric constants. We further define $E[y] = \infty$ and $E_h[y_h] = \infty$ whenever $y \notin \mathbb{A}$ and $y_h \notin \mathbb{A}_{h,\delta}^k$, respectively.

2.3. Interpolation onto Continuous Piecewise Polynomials. For several reasons we need to interpolate from the broken energy space $\mathbb{E}(\mathcal{T}_h) := \prod_{T \in \mathcal{T}_h} H^1(T)$ onto the space $\mathring{\mathbb{V}}_h^k := \mathbb{V}_h^k \cap H^1(\Omega)$ of continuous piecewise polynomials of degree $\leq k$. We refer to [3, 11, 13, 15, 17] for such interpolation estimates. We now construct a Cl  ment type interpolation operator $\Pi_h : \mathbb{E}(\mathcal{T}_h) \rightarrow \mathring{\mathbb{V}}_h^k$, thereby extending [3, 11] to $\mathbb{E}(\mathcal{T}_h)$, because of its simplicity and fitness with our application of it.

We construct Π_h in two steps. We first compute the local L^2 projection $P_h : \mathbb{E}(\mathcal{T}_h) \rightarrow \mathbb{V}_h^k$, which for every $v \in \mathbb{E}(\mathcal{T}_h)$ and $T \in \mathcal{T}_h$ reduces to the equation

$$(2.13) \quad P_h v \in \mathbb{V}_h^k(T) : \quad \int_T (P_h v - v)w = 0 \quad \forall w \in \mathbb{V}_h^k(T),$$

where $\mathbb{V}_h^k(D)$ stands for the restriction of functions in \mathbb{V}_h^k to $D \subset \Omega$. We next define the Cl  ment interpolation operator $I_h : \mathbb{V}_h^k \rightarrow \mathring{\mathbb{V}}_h^k$ of [3, 11] as follows. Given the canonical basis functions $\{\phi_i\}_{i=1}^N$ of $\mathring{\mathbb{V}}_h^k$ with supports $\{\omega_i\}_{i=1}^N$ associated with nodes $\{x_i\}_{i=1}^N$, we compute the L^2 -projection of $v \in \mathbb{V}_h^k$ on stars ω_i

$$v_i \in \mathring{\mathbb{V}}_h^k(\omega_i) : \quad \int_{\omega_i} (v - v_i)w = 0 \quad \forall w \in \mathring{\mathbb{V}}_h^k(\omega_i),$$

and define $I_h v := \sum_{i=1}^N v_i(x_i)\phi_i \in \mathring{\mathbb{V}}_h^k$ and $\Pi_h := I_h \circ P_h : \mathbb{E}(\mathcal{T}_h) \rightarrow \mathring{\mathbb{V}}_h^k$.

Lemma 2.1 (interpolation). *The interpolation operator $\Pi_h := I_h \circ P_h : \mathbb{E}(\mathcal{T}_h) \rightarrow \mathring{\mathbb{V}}_h^k$ is invariant in the space $\mathring{\mathbb{V}}_h^k$ and satisfies the following estimate for all $v \in \mathbb{E}(\mathcal{T}_h)$*

$$(2.14) \quad \|\nabla \Pi_h v\|_{L^2(\Omega)} + \|h^{-1}(v - \Pi_h v)\|_{L^2(\Omega)} \lesssim \|\nabla_h v\|_{L^2(\Omega)} + \|h^{-1/2}[v]\|_{L^2(\Gamma_h^0)}.$$

Proof. The operator Π_h is invariant in $\mathring{\mathbb{V}}_h^k$ because so are P_h and I_h . We next examine properties of P_h and I_h separately.

Step 1: Operator P_h . Since P_h is an elementwise L^2 -projection, we easily deduce

$$\|P_h v - v\|_{L^2(T)} + h_T^{1/2} \|P_h v - v\|_{L^2(\partial T)} + h_T \|\nabla P_h v\|_{L^2(T)} \lesssim h_T \|\nabla v\|_{L^2(T)}.$$

Given a face $e \in \mathcal{E}_h^0$ let $T^\pm \in \mathcal{T}_h$ be the two elements that satisfy $e = T^+ \cap T^-$ and v^\pm the restrictions of v to T^\pm . If $\omega(e) := T^+ \cup T^-$, a simple calculation now shows

$$\begin{aligned} \|[P_h v]\|_{L^2(e)} &\leq \|P_h v^+ - v^+\|_{L^2(e)} + \|P_h v^- - v^-\|_{L^2(e)} + \|v^+ - v^-\|_{L^2(e)} \\ &\lesssim h_e^{1/2} \|\nabla_h v\|_{L^2(\omega(e))} + \|[v]\|_{L^2(e)}. \end{aligned}$$

Step 2: Operator I_h . We recall (see e.g. [11]) that to prove the estimate

$$\|\nabla I_h v\|_{L^2(T)} + \|h^{-1}(I_h v - v)\|_{L^2(T)} \lesssim \|\nabla_h v\|_{L^2(\omega(T))} + \|h^{-1/2}[v]\|_{L^2(\gamma^0(\omega(T)))}$$

for all $v \in \mathbb{V}_h^k$, it suffices to derive the bounds

$$\|\nabla v_i\|_{L^2(\omega_i)} + \|h^{-1}(v - v_i)\|_{L^2(\omega_i)} \lesssim \|\nabla_h v\|_{L^2(\omega_i)} + \|h^{-1/2}[v]\|_{L^2(\gamma_i^0)};$$

hereafter $\gamma^0(\omega(T))$ and $\gamma_i^0 = \gamma^0(\omega_i)$ stand for the skeletons of the discrete neighborhood $\omega(T)$ of $T \in \mathcal{T}_h$ and the star ω_i (interelement boundaries internal to these sets), whereas the index i corresponds to any of the nodes contained in T (assumed to be closed). Since the dimension of the space $\mathbb{V}_h^k(\omega_i)$ is finite and depends only on shape regularity and dimension d , all norms in $\mathbb{V}_h^k(\omega_i)$ are equivalent and independent of meshsize. We further observe that if the right hand side of the last inequality vanishes, then v is constant in ω_i . The definition of v_i thus gives $v_i = v$

and the left hand side vanishes, thereby showing that the desired estimate is valid. The powers of meshsize result from a standard scaling argument.

Step 3: Operator Π_h . Combining the estimates for P_h and I_h yields

$$\|\nabla \Pi_h v\|_{L^2(\Omega)} \lesssim \|\nabla P_h v\|_{L^2(\Omega)} + \|h^{-1/2}[P_h v]\|_{L^2(\Gamma_h^0)} \lesssim \|\nabla_h v\|_{L^2(\Omega)} + \|h^{-1/2}[v]\|_{L^2(\Gamma_h^0)}.$$

A similar estimate is valid for $\|h^{-1}(v - \Pi_h v)\|_{L^2(\Omega)}$. This concludes the proof. \square

We have written (2.14) in a convenient form for our later application. Note that it only requires that \mathbb{V}_h^k contains piecewise constants and make no reference to the actual polynomial degree k . However, since Π_h is invariant on $\mathring{\mathbb{V}}_h^k$, we may apply (2.14) to $v - p$ where $p \in \mathring{\mathbb{V}}_h^k$ is the best H^1 -approximation of $v \in H^{k+1}(\Omega)$

$$\|v - \Pi_h v\|_{L^2(\Omega)} = \|(v - p) - \Pi_h(v - p)\|_{L^2(\Omega)} \lesssim h \|\nabla(v - p)\|_{L^2(\Omega)} \lesssim h^{k+1} |v|_{H^{k+1}(\Omega)}.$$

Corollary 2.1 (boundary error estimate). *The following estimate is valid*

$$(2.15) \quad \|h^{-1/2}(v - \Pi_h v)\|_{L^2(\partial\Omega)} \lesssim \|\nabla_h v\|_{L^2(\Omega)} + \|h^{-1/2}[v]\|_{L^2(\Gamma_h^0)} \quad \forall v \in \mathbb{E}(\mathcal{T}_h).$$

Proof. Let e be a generic boundary edge, not necessarily in \mathcal{E}_h^b , and $T \in \mathcal{T}_h$ be an adjacent element (i.e. $e \subset \partial T$). The scaled trace inequality reads

$$\|h^{-1/2}(v - \Pi_h v)\|_{L^2(e)} \lesssim \|h^{-1}(v - \Pi_h v)\|_{L^2(T)} + \|\nabla(v - \Pi_h v)\|_{L^2(T)}$$

Adding over e , the desired estimate follows from (2.14). \square

The following Friedrichs inequality is another straightforward application of (2.14); similar estimates are proved in [13, 15]. We observe that the jumps $[v]$ of $v \in \mathbb{E}(\mathcal{T}_h)$ in (2.14) are computed on the interior skeleton Γ_h^0 , but the desired estimate requires control of the trace of v on $\partial_D \Omega$.

Corollary 2.2 (discrete Friedrichs inequality). *Given $v \in \mathbb{E}(\mathcal{T}_h)$ and $g \in H^1(\Omega)$, there holds*

$$\|v\|_{L^2(\Omega)} \lesssim \|\nabla_h v\|_{L^2(\Omega)} + \|h^{-1/2}[v]\|_{L^2(\Gamma_h^0)} + \|g\|_{H^1(\Omega)},$$

where $[v] = v - g$ on $\partial_D \Omega$ and the hidden constant solely depends on Ω .

Proof. We start with a standard form of the Friedrichs inequality for $\Pi_h v \in H^1(\Omega)$

$$\|\Pi_h v\|_{L^2(\Omega)} \lesssim \|\nabla \Pi_h v\|_{L^2(\Omega)} + \|\Pi_h v\|_{L^2(\partial_D \Omega)},$$

where the hidden constant depends only on Ω . This, in conjunction with (2.14) and the scaled trace inequality $\|w\|_{L^2(e)} \lesssim h_T^{-1/2} \|w\|_{L^2(T)} + h_T^{1/2} \|\nabla w\|_{L^2(T)}$ with $w = v - \Pi_h v$ and $e \subset \partial T$, yields

$$\|v\|_{L^2(\Omega)} \lesssim \|\nabla_h v\|_{L^2(\Omega)} + \|h^{-1/2}[v]\|_{L^2(\Gamma_h^0)} + \|v\|_{L^2(\Gamma_h^b)}.$$

We finally add and subtract g in the last term and use again the trace inequality, this time for g over Ω , to deduce the asserted estimate. \square

Upon applying Corollary 2.2 twice, first to $v_h \in \mathbb{V}_h^k(g, \Phi)$ and second to $\nabla_h v_h$, we obtain the following Friedrichs inequality

$$(2.16) \quad \|v_h\|_{L^2(\Omega)} + \|\nabla_h v_h\|_{L^2(\Omega)} \lesssim \|v_h\|_E + \|g\|_{H^1(\Omega)} + \|\Phi\|_{H^1(\Omega)}.$$

2.4. Coercivity of the Discrete Energy. We now prove that the discrete energy (2.11) is coercive with respect to a suitable dG norm. As motivation, we start with a similar coercivity estimate for the continuous case.

Lemma 2.2 (coercivity of E). *Let data (g, Φ, f) satisfy (1.2). For any $y \in \mathbb{V}(g, \Phi)$ there holds*

$$\|y\|_{H^2(\Omega)}^2 \lesssim E[y] + \|g\|_{H^1(\Omega)}^2 + \|\Phi\|_{H^1(\Omega)}^2 + \|f\|_{L^2(\Omega)}^2,$$

where $E[y]$ is defined in (1.4).

Proof. In view of (1.4), we start by deriving estimates for the $L^2(\Omega)$ norm of y . We invoke the Friedrichs inequality for $y - g$ and $\nabla y - \Phi$ to obtain

$$\|y\|_{L^2(\Omega)} \leq \|g\|_{L^2(\Omega)} + \|y - g\|_{L^2(\Omega)} \lesssim \|\nabla y\|_{L^2(\Omega)} + \|g\|_{H^1(\Omega)}$$

and likewise

$$\|\nabla y\|_{L^2(\Omega)} \lesssim \|D^2 y\|_{L^2(\Omega)} + \|\Phi\|_{H^1(\Omega)}.$$

Combining these estimates gives

$$(2.17) \quad \|y\|_{H^1(\Omega)}^2 \leq C \left(\|D^2 y\|_{L^2(\Omega)}^2 + \|g\|_{H^1(\Omega)}^2 + \|\Phi\|_{H^1(\Omega)}^2 \right).$$

As a consequence, for any $\sigma > 0$, we find that

$$\begin{aligned} \|D^2 y\|_{L^2(\Omega)}^2 &= 2E[y] + 2 \int_{\Omega} f y \leq 2E[y] + 2\|f\|_{L^2(\Omega)} \|y\|_{L^2(\Omega)} \\ &\leq 2E[y] + \frac{1}{\sigma} \|f\|_{L^2(\Omega)}^2 + \sigma \|y\|_{L^2(\Omega)}^2 \\ &\leq 2E[y] + \frac{1}{\sigma} \|f\|_{L^2(\Omega)}^2 + C\sigma (\|D^2 y\|_{L^2(\Omega)}^2 + \|g\|_{H^1(\Omega)}^2 + \|\Phi\|_{H^1(\Omega)}^2). \end{aligned}$$

Setting $\sigma = \frac{1}{2C}$, we deduce that

$$\|D^2 y\|_{L^2(\Omega)}^2 \lesssim E[y] + \|g\|_{H^1(\Omega)}^2 + \|\Phi\|_{H^1(\Omega)}^2 + \|f\|_{L^2(\Omega)}^2,$$

which combined with (2.17) gives the asserted estimate. \square

We observe that Friedrichs inequality plays a crucial role in the previous proof to control $y - g$ and $\nabla y - \Phi$, which vanish on $\partial_D \Omega$. At the discrete level we face two difficulties: the lack of regularity that leads to interior jumps for y_h and the Nitsche approach that substitutes the explicit imposition of boundary conditions. This explains the explicit form of Corollary 2.2 (discrete Friedrichs inequality). Moreover, the H^2 -norm is replaced by a suitable dG counterpart: given $y_h \in \mathbb{V}_h^k(g, \Phi)$, let

$$(2.18) \quad \|y_h\|_E^2 := \|D_h^2 y_h\|_{L^2(\Omega)}^2 + \|h^{-1/2} [\nabla_h y_h]\|_{L^2(\Gamma_h)}^2 + \|h^{-3/2} [y_h]\|_{L^2(\Gamma_h)}^2.$$

Notice that $\|\cdot\|_E$ is not a norm because of the presence of g and Φ in (2.8).

Lemma 2.3 (coercivity of E_h). *Let data (g, Φ, f) satisfy (1.2) and $y_h \in \mathbb{V}_h^k(g, \Phi)$. If the penalty parameters γ_0, γ_1 in the discrete energy E_h defined in (2.11) are sufficiently large, then there holds*

$$\|y_h\|_E^2 \lesssim E_h[y_h] + \|g\|_{H^1(\Omega)}^2 + \|\Phi\|_{H^1(\Omega)}^2 + \|f\|_{L^2(\Omega)}^2.$$

Proof. We start with the third term in (2.11), and employ Young's inequality and the inverse estimate $\|h^{1/2} D_h^2 y_h\|_{L^2(\Gamma_h)} \lesssim \|D_h^2 y_h\|_{L^2(\Omega)}$ for any $y_h \in \mathbb{V}_h^k(g, \Phi)$ to arrive at

$$\left| (\{\partial_\mu \nabla_h y_h\}, [\nabla_h y_h])_{L^2(\Gamma_h)} \right| \leq \rho \|D_h^2 y_h\|_{L^2(\Omega)}^2 + \frac{C}{\rho} \|h^{-1/2} [\nabla_h y_h]\|_{L^2(\Gamma_h)}^2,$$

for any $\rho > 0$. We next consider the forth term in (2.11): we first use an inverse inequality for $y_h \in \mathbb{V}_h^k$ to obtain for any $e \in \mathcal{E}_h$

$$\|h^{3/2}\{\partial_\mu \Delta_h y_h\}\|_{L^2(e)} \lesssim h\|D^3 y_h\|_{L^2(\omega(e))} \lesssim \|D^2 y_h\|_{L^2(\omega(e))},$$

where $\omega(e)$ is the union of elements containing e . Hence, Young's inequality yields

$$\left| \left(\{\partial_\mu \Delta_h y_h\}, [y_h] \right)_{L^2(\Gamma_h)} \right| \lesssim \rho \|D_h^2 y_h\|_{L^2(\Omega)}^2 + \frac{C}{\rho} \|h^{-3/2} [y_h]\|_{L^2(\Gamma_h)}^2.$$

We thus see that for appropriate choices of ρ , γ_1 , and γ_0 the above terms can be absorbed into $\frac{1}{2}\|D_h^2 y_h\|_{L^2(\Omega)}^2$, $\frac{\gamma_1}{2}\|h^{-1/2}[\nabla_h y_h]\|_{L^2(\Gamma_h)}^2$, and $\frac{\gamma_0}{2}\|h^{-3/2}[y_h]\|_{L^2(\Gamma_h)}^2$ of $E_h[y_h]$. We finally resort to (2.16) to estimate the forcing term as follows:

$$\left| \int_\Omega f y_h \right| \leq \|f\|_{L^2(\Omega)} \|y_h\|_{L^2(\Omega)} \lesssim \|f\|_{L^2(\Omega)} (\|y_h\|_E + \|g\|_{H^1(\Omega)} + \|\Phi\|_{H^1(\Omega)}).$$

This concludes the proof. \square

3. DISCRETE GRADIENT FLOW

We now design a discrete H^2 -gradient flow to construct discrete minimizers. We first introduce the first variation of the isometry constraint (1.1) at $y \in \mathbb{V}(g, \Phi)$

$$(3.1) \quad L[v; y] = (\nabla v)^T \nabla y + (\nabla y)^T \nabla v = 0 \quad \forall v \in \mathbb{V}(0, \mathbf{0}).$$

This serves to describe the tangent manifold to (1.1) at $y \in \mathbb{V}(g, \Phi)$

$$\mathcal{F}[y] := \{v \in \mathbb{V}(0, \mathbf{0}) : L[v; y] = 0\}.$$

Likewise, we introduce the *discrete linearized isometry constraint* at $y_h \in \mathbb{V}_h^k(g, \Phi)$

$$(3.2) \quad L_T[v_h; y_h] := \int_T (\nabla_h v_h)^T \nabla_h y_h + (\nabla_h y_h)^T \nabla_h v_h = 0 \quad \forall v_h \in \mathbb{V}_h^k(0, \mathbf{0}),$$

which imposes the pointwise equality (3.1) on average over each element $T \in \mathcal{T}_h$. This in turn leads to the subspace $\mathcal{F}_h[y_h]$ of $\mathbb{V}_h^k(0, \mathbf{0})$ defined as

$$\mathcal{F}_h[y_h] := \{v_h \in \mathbb{V}_h^k(0, \mathbf{0}) : L_T[v_h; y_h] = 0 \quad \forall T \in \mathcal{T}_h\}.$$

We finally introduce the discrete H^2 -scalar product for all $v_h, w_h \in \mathbb{V}_h^k(0, \mathbf{0})$

$$\begin{aligned} (w_h, v_h)_{H_h^2} &:= (D_h^2 w_h, D_h^2 v_h)_{L^2(\Omega)} \\ &\quad + (h^{-1/2}[\nabla_h w_h], [\nabla_h v_h])_{L^2(\Gamma_h)} + (h^{-3/2}[w_h], [v_h])_{L^2(\Gamma_h)} \end{aligned}$$

and use $\|\cdot\|_{H_h^2}$ to denote the corresponding discrete H^2 -norm.

We are now in a position to describe the *discrete H^2 gradient flow*. Let $y_h^0 \in \mathbb{V}_h^k(g, \Phi)$ be a suitable initial guess with energy $E_h[y_h^0]$ as small as possible and isometry defect $D_h[y_h^0] \leq \tau$, where $\tau > 0$ is a fictitious time-step to be determined later. Given iterate $y_h^n \in \mathbb{V}_h^k(g, \Phi)$, we seek $y_h^{n+1} := y_h^n + \delta y_h^{n+1}$ with $\delta y_h^{n+1} \in \mathcal{F}_h[y_h^n]$ satisfying

$$(3.3) \quad \tau^{-1}(\delta y_h^{n+1}, v_h)_{H_h^2} + \delta E_h[y_h^n + \delta y_h^{n+1}; v_h] = 0 \quad \forall v_h \in \mathcal{F}_h[y_h^n],$$

where $\delta E_h[y_h^{n+1}; v_h]$ is the variational derivative of E_h at y_h^{n+1} in the direction of v_h . This is the Euler-Lagrange equation for a minimizer of the energy

$$\mathcal{F}_h[y_h^n] \ni w_h \mapsto \frac{1}{2\tau} \|\|w_h\|\|_{H_h^2}^2 + E_h[y_h^n + w_h].$$

We thus minimize $E_h[y_h^n + w_h]$ but penalizing the deviation from zero of w_h in the discrete H^2 -norm $|||\cdot|||_{H_h^2}$. In view of (2.10) and (2.11), (3.3) is equivalent to

$$(3.4) \quad \tau^{-1}(\delta y_h^{n+1}, v_h)_{H_h^2} + a_h(\delta y_h^{n+1}, v_h) = a_h(y_h^n, v_h) + (f, v_h)_{L^2(\Omega)} \quad \forall v_h \in \mathcal{F}_h[y_h^n].$$

Remark 3.1 (solvability of (3.4)). Note that problem (3.4) is linear in δy_h^{n+1} and Lemma 2.3 (coercivity of E_h) with vanishing data (g, Φ, f) yields coercivity of a_h

$$(3.5) \quad a_h(v_h, v_h) \geq \alpha |||v_h|||_{H_h^2}^2 \quad \forall v_h \in \mathbb{V}_h^k(0, \mathbf{0})$$

for some constant α independent of h . Since $0 \in \mathcal{F}_h[y_h^n]$ we infer that $\mathcal{F}_h[y_h^n] \neq \emptyset$ and the Lax-Milgram theorem implies existence and uniqueness of a solution $\delta y_h^{n+1} \in \mathcal{F}_h[y_h^n]$ to each step of the discrete gradient flow (3.3). Whether $\mathcal{F}_h[y_h^n]$ is sufficiently rich is a delicate and open question we will touch upon in Section 7.

We now show that the discrete H^2 gradient flow (3.3) reduces the energy E_h .

Lemma 3.2 (energy decay). *Let $y_h^n \in \mathbb{V}_h^k(g, \Phi)$ be the n -th iterate of the discrete H^2 gradient flow (3.3) with data (g, Φ, f) obeying (1.2). If $\delta y_h^{n+1} \neq 0$ is the solution of (3.3), then $y_h^{n+1} = y_h^n + \delta y_h^{n+1}$ satisfies*

$$E_h[y_h^{n+1}] < E_h[y_h^n].$$

Moreover, if α is the coercivity constant in (3.5) and τ is the time step, then

$$(3.6) \quad \left(\frac{\alpha}{2} + \frac{1}{\tau}\right) \sum_{n=0}^{N-1} |||\delta y_h^{n+1}|||_{H_h^2}^2 + E_h[y_h^N] \leq E_h[y_h^0].$$

Proof. We set $v_h = \delta y_h^{n+1}$ in (3.3) and use the fact that E_h is quadratic to obtain

$$\delta E_h[y_h^k + \delta y_h^{n+1}, \delta y_h^{n+1}] = E_h[y_h^{k+1}] - E_h[y_h^k] + \frac{1}{2} a_h(\delta y_h^{n+1}, \delta y_h^{n+1}).$$

Invoking the coercivity property (3.5) we thus get

$$\left(\frac{\alpha}{2} + \frac{1}{\tau}\right) |||\delta y_h^{n+1}|||_{H_h^2}^2 + E_h[y_h^{k+1}] \leq E_h[y_h^k],$$

whence $E_h[y_h^{k+1}] < E_h[y_h^k]$ if $\delta y_h^{n+1} \neq 0$. We finally sum over n to deduce (3.6). \square

We now show that the discrete H^2 -gradient flow guarantees the discrete isometry defect (1.6) for any $\delta > 0$ provided the time step τ is suitably chosen. This is an instance where the nature of the discrete H^2 -scalar product in (3.3) plays a crucial role and is responsible for the next statement.

Lemma 3.3 (discrete isometry defect). *Let the initial guess $y_h^0 \in \mathbb{V}_h^k(g, \Phi)$ for (3.4) be an approximate isometry in the sense that*

$$(3.7) \quad D_h[y_h^0] = \sum_{T \in \mathcal{T}_h} \int_T |(\nabla_h y_h^0)^T \nabla_h y_h^0 - I| \leq \tau,$$

and let

$$(3.8) \quad \delta_0 := (1 + C_F E_h[y_h^0]) \tau,$$

where C_F is the Friedrichs constant hidden in (2.16) for $g = 0$ and $\Phi = 0$. Then every iterate y_h^n of (3.3) satisfies the discrete isometry defect (1.6) for $\delta \geq \delta_0$

$$(3.9) \quad D_h[y_h^n] = \sum_{T \in \mathcal{T}_h} \left| \int_T (\nabla_h y_h^n)^T \nabla_h y_h^n - I \right| \leq \delta.$$

Proof. We start by quantifying the increase of the discrete isometry defect in each iteration of the discrete gradient flow. Upon rewriting the linearized isometry constraint $L_T[v_h; y_h^{n+1}] = 0$ in (3.2) with $v_h = \delta y_h^{n+1}$ and $y_h^{n+1} = y_h^n + \delta y_h^{n+1}$ as

$$\int_T (\nabla_h y_h^{n+1})^T \nabla_h y_h^{n+1} = \int_T (\nabla_h y_h^n)^T \nabla_h y_h^n + \int_T (\nabla_h \delta y_h^{n+1})^T \nabla_h \delta y_h^{n+1},$$

summing for $n = 0$ to $n = N - 1$, and exploiting telescopic cancellation, we obtain

$$\int_T (\nabla_h y_h^N)^T \nabla_h y_h^N = \int_T (\nabla_h y_h^0)^T \nabla_h y_h^0 + \sum_{n=0}^{N-1} \|\nabla_h \delta y_h^{n+1}\|_{L^2(T)}^2.$$

Consequently, adding over $T \in \mathcal{T}_h$ and employing (3.7), we deduce

$$D_h[y_h^N] = \sum_{T \in \mathcal{T}_h} \left| \int_T (\nabla_h y_h^N)^T \nabla_h y_h^N - I \right| \leq \tau + \sum_{n=0}^{N-1} \|\nabla_h \delta y_h^{n+1}\|_{L^2(\Omega)}^2.$$

We finally combine the energy decay relation (3.6) with the H^2 -type Friedrichs inequality (2.16) for $g = 0$ and $\Phi = 0$ to get

$$\sum_{n=0}^{N-1} \|\nabla_h \delta y_h^{n+1}\|_{L^2(\Omega)}^2 \leq C_F \sum_{n=0}^{N-1} \|\delta y_h^{n+1}\|_{H_h^2}^2 < C_F E_h[y_h^0] \tau.$$

Inserting this in the bound for $D_h[y_h^N]$ yields the asserted estimate (3.9). \square

Remark 3.4 (choice of initial guess y_h^0). We realize from Lemma 3.3 (discrete isometry defect) that choosing y_h^0 might be tricky, unless we can make the discrete isometry defect $D_h[y_h^0]$ small without increasing much the discrete energy $E_h[y_h^0]$. We will revisit this issue in Section 6.

4. DISCRETE HESSIAN

In this section we provide a suitable definition of discrete Hessian $H_h[y_h]$ for $y_h \in \mathbb{V}_h^k$. Central to this concept is the following question: if the discontinuous function y_h converges strongly in $[L^2(\Omega)]^3$ to $y \in [H^2(\Omega)]^3$, under what conditions could $H_h[y_h]$ converge weakly in $[L^2(\Omega)]^{3 \times 2 \times 2}$ to $D^2 y$?

$$(4.1) \quad H_h[y_h] \rightharpoonup D^2 y \quad \text{in} \quad [L^2(\Omega)]^{3 \times 2 \times 2}.$$

It is apparent that the information contained in the broken gradient $D_h^2 y_h \in [L^2(\Omega)]^{3 \times 2}$ is insufficient for this purpose, and that the jumps $[y_h] \in [L^2(\Gamma_h)]^3$ and $[\nabla_h y_h] \in [L^2(\Gamma_h)]^{3 \times 2}$ do not provide directly the missing information because they are singular with respect to Lebesgue measure. To bridge this gap, in Section 4.1 we introduce lifting operators of $[y_h]$ and $[\nabla_h y_h]$ and use them to construct $H_h[y_h]$. Another important property of $H_h[y_h]$ critical for the lim-inf argument is

$$(4.2) \quad \frac{1}{2} \|H_h[y_h]\|_{L^2(\Omega)}^2 - (f_h, y_h)_{L^2(\Omega)} \leq E_h[y_h],$$

which is valid with constant 1. We will prove (4.1) and (4.2) in Section 4.2. Our approach is similar to that developed by Pryer [30], so we will be brief.

4.1. Lifting operators and definition of $H_h[y_h]$. We define two lifting operators $R_h([\nabla_h v_h])$ and $B_h([v_h])$ that extend the jumps $[\nabla_h v_h]$ and $[v_h]$ of any $v_h \in \mathbb{V}_h^k$ from the skeleton Γ_h to the bulk Ω . It turns out that of the many ways this can be achieved, there is only one that leads to (4.1) and (4.2). We describe this next. In preparation, we define the space of piecewise Hessians

$$\mathbb{H}_h^k := \{\tau_h \in L_2(\Omega)^{2 \times 2} : \tau_h|_T = D_h^2 w_h, \quad w_h \in \mathbb{V}_h^k(T), \quad T \in \mathcal{T}_h\}.$$

The first lifting operator $R_h := \sum_{e \in \mathcal{E}_h} r_e : L^2(\Gamma_h) \rightarrow \mathbb{H}_h^k$ hinges on the local liftings $r_e : L^2(e) \rightarrow \mathbb{H}_h^k$ which, for all $e \in \mathcal{E}_h$ and $\phi \in [L^2(e)]^2$, are defined by

$$(4.3) \quad \int_{\omega(e)} r_e(\phi) : \tau_h = \int_e \phi \cdot \{\tau_h\} \mu_e \quad \forall \tau_h \in \mathbb{H}_h^k,$$

and vanish outside $\omega(e)$, the patch associated with e . Notice that upon taking $\tau_h = D^2 w_h$, we get

$$(4.4) \quad (R_h([\nabla_h v_h]), D^2 w_h)_{L^2(\Omega)} = ([\nabla_h v_h], \{\partial_\mu(\nabla_h w_h)\})_{L^2(\Gamma_h)} \quad \forall w_h \in \mathbb{V}_h^k.$$

The second lifting operator $B_h := \sum_{e \in \mathcal{E}_h} b_e : L^2(e) \rightarrow \mathbb{H}_h^k$ relies on the local liftings $b_e : L^2(e) \rightarrow \mathbb{H}_h^k$ which, for all $e \in \mathcal{E}_h$ and $\phi \in L^2(e)$, are given by

$$(4.5) \quad \int_{\omega(e)} b_e(\phi) : \tau_h = \int_e \phi \cdot \{\operatorname{div} \tau_h\} \cdot \mu_e \quad \forall \tau_h \in \mathbb{H}_h^k,$$

and vanish outside $\omega(e)$. In this case again taking $\tau_h = D_h^2 w_h$ and observing that

$$\operatorname{div}(D_h^2 v_h) = \nabla_h(\Delta_h v_h)$$

elementwise, we obtain

$$(4.6) \quad (B_h([v_h]), D_h^2 \tau_h) = ([v_h], \{\partial_\mu(\Delta_h w_h)\})_{L^2(\Gamma_h)} \quad \forall w_h \in \mathbb{V}_h^k.$$

We now return to vector-valued functions.

Definition 4.1 (discrete Hessian). We let $H_h : \mathbb{V}_h^k(g, \Phi) \rightarrow [\mathbb{H}_h^k]^3$ be

$$(4.7) \quad H_h[y_h] := D_h^2 y_h - R_h([\nabla_h y_h]) + B_h([y_h]),$$

where $R_h = \sum_{e \in \Gamma_h} r_e$ and $B_h = \sum_{e \in \Gamma_h} b_e$ are defined in (4.3) and (4.5).

It is worth realizing that, in view of (4.4) and (4.6), we readily find

$$\begin{aligned} (H_h[y_h], \tau_h)_{L^2(\Omega)} &= (D_h^2 y_h, \tau_h)_{L^2(\Omega)} \\ &\quad - ([\nabla_h y_h], \{\partial_\mu(\nabla_h w_h)\})_{L^2(\Gamma_h)} + ([y_h], \{\partial_\mu(\Delta_h y_h)\})_{L^2(\Gamma_h)} \end{aligned}$$

for all $\tau_h \in [\mathbb{H}_h^k]^3$, and that the boundary jumps on Γ_h^b are given by $[y_h] = y_h^- - g$ and $[\nabla_h y_h] = \nabla_h y_h^- - \Phi$, according to (2.8).

4.2. Properties of $H_h[y_h]$. We start with L^2 a priori bounds for R_h, B_h and H_h .

Lemma 4.2 (L^2 -bounds of lifting operators). *Let $y_h \in \mathbb{V}_h^k(g, \Phi)$ with data (g, Φ) satisfying (1.2). Then, for all $e \in \Gamma_h$, there holds*

$$\|r_e([\nabla_h y_h])\|_{L^2(\omega(e))} \lesssim \|h^{-1/2}[\nabla_h y_h]\|_{L^2(e)}$$

and

$$\|b_e([y_h])\|_{L^2(\omega(e))} \lesssim \|h^{-3/2}[y_h]\|_{L^2(e)}.$$

Proof. We argue as in [16] but with emphasis on boundary edges $e \in \mathcal{E}_h^b$ because they contain the Dirichlet data (g, Φ) according to (2.8); see also [11, 19, 30]. We prove the first bound because the other one is identical. Definition (4.3) of r_e yields

$$\|r_e(\nabla_h y_h - \Phi)\|_{L^2(\omega(e))}^2 = \int_e \{r_e(\nabla_h y_h - \Phi)\} \mu_e \cdot (\nabla_h y_h - \Phi).$$

Combining (2.9) with an inverse estimate implies

$$\begin{aligned} \|r_e(\nabla_h y_h - \Phi)\|_{L^2(\omega(e))}^2 &\leq \|h^{1/2} r_e(\nabla_h y_h - \Phi)\|_{L^2(e)} \|h^{-1/2} (\nabla_h y_h - \Phi)\|_{L^2(e)} \\ &\lesssim \|r_e(\nabla_h y_h - \Phi)\|_{L^2(\omega(e))} \|h^{-1/2} (\nabla_h y_h - \Phi)\|_{L^2(e)}. \end{aligned}$$

Since the same argument applies to interior edges $e \in \mathcal{E}_h^0$, with $\nabla_h y_h - \Phi$ replaced by $[\nabla_h y_h]$ defined in (2.7), the proof is complete. \square

For each quadrilateral (resp. triangle) $T \in \mathcal{T}_h$ there are 4 (resp. 3) sets $\omega(e)$ with non-empty intersection, we immediately get the following global bounds

$$(4.8) \quad \begin{aligned} \|R_h([\nabla_h y_h])\|_{L^2(\Omega)} &\lesssim \|h^{-1/2} [\nabla_h y_h]\|_{L^2(\Gamma_h)}, \\ \|B_h([y_h])\|_{L^2(\Omega)} &\lesssim \|h^{-3/2} [y_h]\|_{L^2(\Gamma_h)}, \end{aligned}$$

as well as the following corollary.

Corollary 4.1 (L^2 bound of discrete Hessian). *If $y_h \in \mathbb{V}_h^k(g, \Phi)$ with data (g, Φ) satisfying (1.2), then the following bound holds*

$$\|H_h[y_h]\|_{L^2(\Omega)} \lesssim \|y_h\|_E.$$

Proof. Combine Definition 4.1 (discrete Hessian) with the above global bounds. \square

While there is some flexibility in the definitions (4.3) and (4.5) of lifts r_e and b_e for Lemma 4.2 (L^2 -bounds of lifting operators) to be valid, the following result reveals that these definitions are just right for weak convergence of $H_h[y_h]$. This is crucial for the lim-sup inequality for E_h in Section 5.3. We refer to [30] for a similar result for any Lebesgue exponent p .

Proposition 4.3 (weak convergence of $H_h[y_h]$). *Let $y_h \in \mathbb{V}_h^k(g, \Phi)$ with data (g, Φ) satisfying (1.2). If $\|y_h\|_E \leq C$ for all h and y_h converges to a function $y \in [H^2(\Omega)]^3$ in $[L^2(\Omega)]^3$ as $h \rightarrow 0$, then*

$$H_h[y_h] \rightharpoonup D^2 y \quad \text{in} \quad [L^2(\Omega)]^{3 \times 2 \times 2}.$$

Proof. We need to show that

$$\int_{\Omega} H_h[y_h] : \tau \rightarrow \int_{\Omega} D^2 y : \tau \quad \text{as } h \rightarrow 0$$

for all $\tau \in [C_0^\infty(\Omega)]^{3 \times 2 \times 2}$. To this end, we argue with each component of y_h , integrate by parts elementwise and utilize the definition (4.7) of $H_h[y_h]$ to deduce

$$\begin{aligned} \int_{\Omega} H_h[y_h] : \tau &= \sum_{T \in \mathcal{T}_h} \int_T y_h \cdot \operatorname{div} \operatorname{div} \tau \\ &\quad - \sum_{e \in \mathcal{E}_h} \int_{\omega(e)} r_e[\nabla y_h] : (\tau - \tau_h) + \sum_{e \in \mathcal{E}_h} \int_{\omega(e)} b_e[y_h] : (\tau - \tau_h) \\ &\quad + \sum_{e \in \mathcal{E}_h^0} \int_e [\nabla_h y_h] \cdot \{\tau - \tau_h\} \mu_e - \sum_{e \in \mathcal{E}_h^0} \int_e [y_h] \{\operatorname{div}(\tau - \tau_h)\} \mu_e \\ &\quad + \sum_{e \in \mathcal{E}_h^b} \int_e (y_h - g) \{\operatorname{div} \tau_h\} \mu_e \end{aligned}$$

where $\tau_h \in [\mathbb{V}_h^k \cap H_0^1(\Omega)]^{3 \times 2 \times 2}$ is the Lagrange interpolant of τ . We point out that even though τ and τ_h have vanishing traces, there is a contribution of boundary terms $e \in \mathcal{E}_h^b$ because they appear in Definition 4.1 (discrete Hessian). In view of the uniform bound $\|y_h\|_E \leq C$ and Lemma 4.2, we deduce

$$\begin{aligned} \|R_h([\nabla_h y_h])\|_{L^2(\Omega)} + \|B_h([y_h])\|_{L^2(\Omega)} &\leq C, \\ \|h^{-1/2}(\nabla_h y_h - \Phi)\|_{L^2(\Gamma_h^b)} + \|h^{-3/2}(y_h - g)\|_{L^2(\Gamma_h^b)} &\leq C. \end{aligned}$$

Since $\tau_h \rightarrow \tau$ in $[H^1(\Omega)]^{3 \times 2 \times 2}$ and $y_h \rightarrow y$ in $[L^2(\Omega)]^3$, we obtain

$$\int_{\Omega} H_h[y_h] : \tau \rightarrow \int_{\Omega} y : \operatorname{div} \operatorname{div} \tau = \int_{\Omega} D^2 y : \tau$$

as $h \rightarrow 0$ because $y \in [H^2(\Omega)]^3$. This is the asserted limit. \square

Another consequence of Definition 4.1 (discrete Hessian) and Lemma 4.2 (L^2 -bounds of lifting operators) is (4.2) with constant 1. This is crucial for the rest.

Proposition 4.4 (relation between $E_h[y_h]$ and $H_h[y_h]$). *Let data (g, Φ, f) satisfy (1.2) and $y_h \in \mathbb{V}_h^k(g, \Phi)$. Then the discrete energy $E_h[y_h]$ of y_h defined in (2.11) and the discrete Hessian of y_h defined in (4.7) satisfy*

$$\frac{1}{2} \|H_h[y_h]\|_{L^2(\Omega)}^2 - (f, y_h)_{L^2(\Omega)} \leq E_h[y_h],$$

provided the penalty parameters γ_0 and γ_1 are chosen sufficiently large.

Proof. We expand the expression for $H_h[y_h]$ and utilize (4.4) and (4.6) to obtain

$$(4.9) \quad \frac{1}{2} \int_{\Omega} |H_h(y_h)|^2 - \int_{\Omega} f y_h = E_h[y_h] + I_h,$$

where

$$\begin{aligned} I_h &:= \frac{1}{2} \|B_h([y_h]) - R_h([\nabla_h y_h])\|_{L^2(\Omega)}^2 \\ &\quad - \gamma_0 \|h^{-3/2}[y_h]\|_{L^2(\Gamma_h)}^2 - \gamma_1 \|h^{-1/2}[\nabla_h y_h]\|_{L^2(\Gamma_h)}^2. \end{aligned}$$

In view of (4.8) there is a constant C independent of h such that

$$I_h \leq (C - \gamma_0) \|h^{-3/2}[y_h]\|_{L^2(\Gamma_h)}^2 + (C - \gamma_1) \|h^{-1/2}[\nabla_h y_h]\|_{L^2(\Gamma_h)}^2 \leq 0$$

for γ_0 and γ_1 sufficiently large. This is what we intended to prove. \square

It is convenient to point out, for later use, that γ_0, γ_1 large also yield

$$(4.10) \quad I_h \leq -\frac{1}{2} \|h^{-3/2}[y_h]\|_{L^2(\Gamma_h)}^2 - \frac{1}{2} \|h^{-1/2}[\nabla_h y_h]\|_{L^2(\Gamma_h)}^2.$$

5. Γ -CONVERGENCE OF E_h

In this section we prove the Γ -convergence of E_h to E . To this end, we prove a lim-inf inequality for E_h using a compactness argument for $y_h \in \mathbb{A}_{h,\delta}^k(g, \Phi)$ with uniformly bounded energies, combined with results from Section 4. We also prove a lim-sup inequality upon constructing a recovery sequence for any $y \in \mathbb{A}(g, \Phi)$ using a simple regularization argument and interpolation. These two results imply Γ -convergence of E_h as well as convergence (up to a subsequence) of global minimizers of E_h in $\mathbb{A}_{h,\delta}^k(g, \Phi)$ to a global minimizer of E in $\mathbb{A}(g, \Phi)$. Lastly, we combine these results to show that the stabilization terms

$$\|h^{-3/2}[y_h]\|_{L^2(\Gamma_h)} \rightarrow 0, \quad \|h^{-1/2}[\nabla_h y_h]\|_{L^2(\Gamma_h)} \rightarrow 0 \quad \text{as } h \rightarrow 0,$$

for such sequence of minimizers and that the convergence of $H_h[y_h]$ in Proposition 4.3 (weak convergence of $H_h[y_h]$) is, in fact, strong in $[L^2(\Omega)]^{3 \times 2 \times 2}$.

5.1. Equi-coercivity and compactness. If data (g, Φ, f) satisfies (1.2) and $y_h \in \mathbb{V}_h^k(g, \Phi)$ possesses a uniform bound $E_h[y_h] \leq C$ for all $h > 0$, then Lemma 2.3 (coercivity of E_h) guarantees *equi-coercivity*

$$(5.1) \quad \|y_h\|_E^2 \lesssim E_h[y_h] + \|g\|_{H^1(\Omega)}^2 + \|\Phi\|_{H^1(\Omega)}^2 + \|f\|_{L^2(\Omega)}^2 \leq C.$$

This, together with Friedrichs estimate (2.16), leads to weakly converging sequences.

We now establish the L^2 -compactness property.

Proposition 5.1 (compactness in $L^2(\Omega)$). *Let the sequence $\{y_h\}_{h>0} \subset \mathbb{A}_{h,\delta}^k$ satisfy the uniform bound $E_h[y_h] \leq \Lambda$ for all $h > 0$ with Λ independent of h . Then there exists a subsequence (not relabeled) and a function $y \in \mathbb{V}(g, \Phi)$ such that $y_h \rightarrow y$ in $[L^2(\Omega)]^3$ as $h, \delta \rightarrow 0$. Moreover, the discrete Hessian $H_h[y_h]$ converges to D^2y weakly in $[L^2(\Omega)]^3$.*

Proof. We proceed in several steps.

Step 1 (weak convergence in L^2). We first use (5.1) to deduce that $\|y_h\|_E \lesssim 1$ for all h . We next employ the Friedrichs inequality (2.16) to obtain $\|y_h\|_{L^2(\Omega)} \lesssim 1$ for all h . Consequently, there exists a subsequence of $\{y_h\}_{h>0}$ (not relabeled) converging weakly in $[L^2(\Omega)]^3$ to some $y \in [L^2(\Omega)]^3$. We must show that $y \in \mathbb{V}(g, \Phi)$.

Step 2 (H^1 regularity of y and L^2 strong convergence). To prove that $y \in [H^1(\Omega)]^3$ we need to regularize y_h . To this end, we employ the smoothing interpolation operator Π_h defined in Section 2.3 and let $z_h := \Pi_h y_h \in \mathring{\mathbb{V}}_h^k = \mathbb{V}_h^k \cap H_0^1(\Omega)$. In view of the stability bound (2.14) and the Friedrichs H^2 -type estimate (2.16), we find that

$$\begin{aligned} \|z_h\|_{L^2(\Omega)} + \|\nabla z_h\|_{L^2(\Omega)} &\lesssim \|y_h\|_{L^2(\Omega)} + \|\nabla_h y_h\|_{L^2(\Omega)} + \|h^{-1/2}[y_h]\|_{L^2(\Gamma_h^0)} \\ &\lesssim \|y_h\|_E + \|g\|_{H^1(\Omega)} + \|\Phi\|_{H^1(\Omega)}. \end{aligned}$$

Equi-coercivity property (5.1) implies that z_h is uniformly bounded in H^1 . Consequently, (a subsequence of) z_h converges weakly to some $z \in [H^1(\Omega)]^3$ and strongly

to z in $[L^2(\Omega)]^3$ and $[L^2(\partial_D\Omega)]^3$. Property (2.14) of Π_h yields

$$\begin{aligned} \|y_h - z\|_{L^2(\Omega)} &\leq \|y_h - \Pi_h y_h\|_{L^2(\Omega)} + \|z - z_h\|_{L^2(\Omega)} \\ &\lesssim h \left(\|\nabla_h y_h\|_{L^2(\Omega)} + \|h^{-1/2}[y_h]\|_{L^2(\Gamma_h^0)} \right) + \|z - z_h\|_{L^2(\Omega)} \rightarrow 0 \end{aligned}$$

as $h \rightarrow 0$ because of the previous bound. The uniqueness of the weak $L^2(\Omega)$ limit implies that $y = z \in [H^1(\Omega)]^3$ and that y_h converges to y strongly in $[L^2(\Omega)]^3$. Regarding the boundary condition, we first observe that

$$\|h^{-3/2}(y_h - g)\|_{L^2(\partial_D\Omega)} = \|h^{-3/2}[y_h]\|_{L^2(\Gamma_h^b)} \leq E_h[y_h] \lesssim 1,$$

whence $\|y_h - g\|_{L^2(\partial_D\Omega)} \rightarrow 0$ as $h \rightarrow 0$, and next that

$$z - g = (z - z_h) + (\Pi_h y_h - y_h) + (y_h - g).$$

Since the middle term satisfies $\|\Pi_h y_h - y_h\|_{L^2(\partial_D\Omega)} \rightarrow 0$ as $h \rightarrow 0$, in view of Corollary 2.1 (boundary error estimate) and (5.1), we infer that $y = z = g$ on $\partial_D\Omega$.

Step 3 (H^2 regularity of y and H^1 strong convergence). We repeat Step 2 with $\nabla_h y_h$. We thus define $Z_h := \Pi_h \nabla_h y_h \in [\mathring{V}_h^k]^{3 \times 2}$. Applying again the stability bound (2.14) in conjunction with (5.1) gives the uniform bound

$$\|Z_h\|_{L^2(\Omega)} + \|\nabla Z_h\|_{L^2(\Omega)} \lesssim \|\nabla_h y_h\|_{L^2(\Omega)} + \|D_h^2 y_h\|_{L^2(\Omega)} + \|h^{-1/2}[\nabla_h y_h]\|_{L^2(\Gamma_h^0)} \leq C.$$

Hence, Z_h converges weakly in $[H^1(\Omega)]^{3 \times 2}$ and strongly in $[L^2(\Omega)]^{3 \times 2}$ to a function $Z \in [H^1(\Omega)]^{3 \times 2}$. Moreover, an argument similar to Step 2, again relying on Corollary 2.1, yields $Z = \Phi$ on $\partial_D\Omega$ and $\|\nabla_h y_h - Z\|_{L^2(\Omega)} \rightarrow 0$ as $h \rightarrow 0$.

It remains to show that $Z = \nabla y$, whence $y \in [H^2(\Omega)]^3$. For any test function $\phi \in [C_0^\infty(\Omega)]^{3 \times 2}$, elementwise integration by parts leads to

$$\int_{\Omega} \nabla_h y_h : \phi = - \int_{\Omega} y_h \cdot \operatorname{div} \phi + \int_{\Gamma_h^0} [y_h] \cdot \phi \mu.$$

We next show that the last term tends to 0 as $h \rightarrow 0$, which in turn implies

$$\int_{\Omega} Z : \phi = - \int_{\Omega} y \cdot \operatorname{div} \phi,$$

or equivalently $Z = \nabla y$. In fact, note that

$$\left| \int_{\Gamma_h^0} [y_h] \cdot \phi \mu \right| \lesssim \|h^{-1/2}[y_h]\|_{L^2(\Gamma_h^0)} \|h^{1/2}\phi\|_{L^2(\Gamma_h^0)} \rightarrow 0 \quad \text{as } h \rightarrow 0,$$

because $\|h^{-1/2}[y_h]\|_{L^2(\Gamma_h)} \leq h\|y_h\|_E \rightarrow 0$ while $\|h^{1/2}\phi\|_{L^2(\Gamma_h^0)} \lesssim |\Omega|\|\phi\|_{L^\infty(\Omega)} \leq C$.

Step 4 (isometry constraint). To show that y satisfies (1.1), we combine the discrete isometry defect (1.6), which controls the isometry constraint mean over elements, with the discrete Hessian, which controls oscillations of $\nabla_h y_h$. In fact, we prove

$$(5.2) \quad \sum_{T \in \mathcal{T}_h} \|(\nabla_h y_h)^T \nabla_h y_h - I\|_{L^1(T)} \lesssim h + \delta.$$

Let J_T denote the isometry constraint mean over $T \in \mathcal{T}_h$

$$J_T := |T|^{-1} \int_T \left((\nabla_h y_h)^T \nabla_h y_h - I \right),$$

and write

$$\|(\nabla_h y_h)^T \nabla_h y_h - I\|_{L^1(T)} \leq \|((\nabla_h y_h)^T \nabla_h y_h - I) - J_T\|_{L^1(T)} + \|J_T\|_{L^1(T)}.$$

For the second term, we employ (1.6) to see that

$$\|J_T\|_{L^1(T)} = |T| |J_T| \Rightarrow \sum_{T \in \mathcal{T}_h} |T| |J_T| = D_h[y_h] \leq \delta.$$

For the first term, instead, we apply a Poincaré-Friederich inequality in $L^1(T)$ to obtain

$$\begin{aligned} \|((\nabla_h y_h)^T \nabla_h y_h - I) - J_T\|_{L^1(T)} &\lesssim h \|\nabla_h((\nabla_h y_h)^T \nabla_h y_h)\|_{L^1(T)} \\ &\lesssim h \|D_h^2 y_h\|_{L^2(T)} \|\nabla_h y_h\|_{L^2(T)}. \end{aligned}$$

Summing over $T \in \mathcal{T}_h$ and using the H^2 -type Friedrichs inequality (2.16), together with Lemma 2.3 (coercivity of $E_h[y_h]$) and the uniform bound on $E_h[y_h]$, we get

$$\sum_{T \in \mathcal{T}_h} \|((\nabla_h y_h)^T \nabla_h y_h - I) - J_T\|_{L^1(T)} \lesssim h \sum_{T \in \mathcal{T}_h} \|D_h^2 y_h\|_{L^2(T)} \|\nabla_h y_h\|_{L^2(T)} \lesssim h,$$

whence (5.2) follows; the hidden constant depends on Λ and data (g, Φ, f) .

With this at hand, we now show that $\|\nabla y^T \nabla y - I\|_{L^1(\Omega)} = 0$. We observe

$$\nabla y^T \nabla y - I = \nabla y^T (\nabla y - \nabla_h y_h) + (\nabla y^T - (\nabla_h y_h)^T) \nabla_h y_h + (\nabla_h y_h)^T \nabla_h y_h - I,$$

which implies

$$\|\nabla y^T \nabla y - I\|_{L^1(\Omega)} \lesssim \left(\|\nabla y\|_{L^2(\Omega)} + \|\nabla_h y_h\|_{L^2(\Omega)} \right) \|\nabla_h y_h - \nabla y\|_{L^2(\Omega)} + h + \delta \rightarrow 0$$

as $h, \delta \rightarrow 0$, upon recalling the strong convergence of $\nabla_h y_h$ to ∇y in $[L^2(\Omega)]^{3 \times 2}$ from Step 3 and the uniform bound of $\nabla_h y_h$ in $[L^2(\Omega)]^{3 \times 2}$.

Step 6 (weak convergence of $H_h[y_h]$). This follows from Proposition 4.3 (weak convergence of $H_h[y_h]$) because $y_h \rightarrow y$ strongly in $[L^2(\Omega)]^3$, the regularity property $y \in [H^2(\Omega)]^3$, and the equi-coercivity bound (5.1). The proof is thus complete. \square

5.2. Lim-inf property of E_h . The lim-inf property follows from the preceding results, but we prove it here separately to highlight it. Instead of looking at a general sequence $\{y_h\}_{h>0}$ with $y_h \rightarrow y$ in $[L^2(\Omega)]^3$, we assume $E_h[y_h] \leq \Lambda$ for all h and uniform constant $\Lambda > 0$, since otherwise the lim-inf inequality is trivial.

Lemma 5.2 (lim-inf property). *Let the penalty parameters γ_0 and γ_1 in (2.11) be chosen sufficiently large, and let the discrete isometry defect parameter $\delta = \delta(h) \rightarrow 0$ as $h \rightarrow 0$. Let $y_h \in \mathbb{A}_{h,\delta}^k$ and $E_h[y_h] \leq \Lambda$ for all h with Λ independent of h . Then, there exists $y \in \mathbb{A}$ such that $y_h \rightarrow y$ in $[L^2(\Omega)]^3$ as $h \rightarrow 0$ and*

$$E[y] \leq \liminf_{h \rightarrow 0} E_h[y_h].$$

Proof. Since $y_h \in \mathbb{A}_{h,\delta}^k$ and $E_h[y_h] \leq \Lambda$, we invoke Proposition 5.1 (compactness in $L^2(\Omega)$) to get $y \in \mathbb{A}$ that satisfies the boundary conditions and the isometry constraint as well as

$$y_h \rightarrow y, \quad H_h[y_h] \rightharpoonup D^2 y,$$

in $L^2(\Omega)$. We use the lower-semicontinuity of the L^2 -norm and the fact that $(f, y_h)_{L^2(\Omega)} \rightarrow (f, y)_{L^2(\Omega)}$ as $h \rightarrow 0$ to derive

$$\frac{1}{2} \int_{\Omega} |D^2 y|^2 - \int_{\Omega} f y \leq \frac{1}{2} \liminf_{h \rightarrow 0} \left(\int_{\Omega} |H_h(y_h)|^2 - \int_{\Omega} f y_h \right).$$

We next employ Proposition 4.4 (L^2 -bound of H_h with respect to E_h), i.e.

$$\frac{1}{2} \int_{\Omega} |H_h(y_h)|^2 - \int_{\Omega} f y_h \leq E_h[y_h],$$

and combine the two inequalities to deduce the asserted estimate. \square

5.3. Lim-sup property of E_h . We now prove the second inequality that is necessary for the Γ -convergence of E_h . Since we are interested in minimizers of E within the admissible set \mathbb{A} , we prove the existence of a recovery sequence in $[L^2(\Omega)]^3$ for a function $y \in \mathbb{A}$ via regularization and Lagrange interpolation. Since the isometry and Dirichlet boundary constraints are relaxed via (1.6) and the Nitsche's approach, we do not need to preserve them in the regularization and interpolation procedures. This extra flexibility is an improvement over [5, 8], where the lim-sup property is proven under the assumption that both procedures preserve those constraints using an intricate approximation argument by P. Hornung [25].

Lemma 5.3 (lim-sup property). *Let the penalty parameters γ_0 and γ_1 in (2.11) be sufficiently large. For any $y \in \mathbb{A}$, there exists a recovery sequence $\{y_h\}_h \subset \mathbb{A}_{h,\delta}^k \cap [H^1(\Omega)]^{3 \times 2}$ with $\|D_h^2 y_h\|_{L^2(\Omega)} \lesssim \|y\|_{H^2(\Omega)}$ uniformly for each h such that*

$$y_h \rightarrow y \quad \text{in} \quad [L^2(\Omega)]^3$$

and

$$E[y] \geq \limsup_{h,\delta \rightarrow 0} E_h[y_h],$$

provided $h \leq 1$ and $\delta \geq \delta_1$ where

$$(5.3) \quad \delta_1 := Ch \|y\|_{H^2(\Omega)}^2$$

and C is an interpolation constant that depends on the shape regularity of $\{\mathcal{T}_h\}_h$.

Proof. We proceed in several steps.

Step 1 (recovery sequence). Let $\Lambda := \|y\|_{H^2(\Omega)}$ and let $y_h := I_h^k y \in [\mathring{\mathbb{V}}_h^k]^3 = [\mathbb{V}_h^k \cap H^1(\Omega)]^3$ be the standard Lagrange interpolant of y , which is well-defined in \mathbb{R}^2 because $H^2(\Omega) \subset C^0(\bar{\Omega})$. We first show that $D_h^2 y_h$ is uniformly in $[L^2(\Omega)]^{3 \times 2 \times 2}$; in fact, we show an elementwise stability estimate for any $T \in \mathcal{T}_h$. If \hat{T} is the reference element, the (generally non-affine) iso-parametric mapping $F_T : \hat{T} \rightarrow T$ induces the relation $\hat{z} = z \circ F_T$ for any function $z \in H^2(T)$ and corresponding estimate [18, 21]

$$h_T^{-1} \|D^2 z\|_{L^2(T)} \lesssim \|DF_T^{-1}\|_{L^\infty(T)}^2 \|D^2 \hat{z}\|_{L^2(\hat{T})} + \|D^2 F_T^{-1}\|_{L^\infty(T)} \|D \hat{z}\|_{L^2(\hat{T})}.$$

Since $\|D^2 F_T^{-1}\|_{L^\infty(T)} \lesssim \|DF_T^{-1}\|_{L^\infty(T)}^2$ [18, 21], we deduce

$$\|D^2 z\|_{L^2(T)} \lesssim h_T \|DF_T^{-1}\|_{L^\infty(\hat{T})}^2 \|\hat{z}\|_{H^2(\hat{T})}.$$

Likewise, the following reverse inequality is valid

$$\|D^2 \hat{z}\|_{L^2(\hat{T})} \lesssim h_T^{-1} \|DF_T\|_{L^\infty(\hat{T})}^2 \|z\|_{H^2(T)}.$$

We next observe that it suffices to prove $\|D^2(y - I_h y)\|_{L^2(T)} \lesssim \|y\|_{H^2(T)}$ by triangle inequality. Let $z = y - I_h y \in [H^2(T)]^3$ and apply the preceding estimate to obtain

$$(5.4) \quad \|D^2(y - I_h y)\|_{L^2(T)} \lesssim h_T \|DF_T^{-1}\|_{L^\infty(T)}^2 \|\hat{y} - \hat{I}\hat{y}\|_{H^2(\hat{T})},$$

where \hat{I} is the Lagrange interpolation operator and $\hat{I}\hat{y} = (I_h y) \circ F_T \in \mathbb{Q}_k$ or \mathbb{P}_k . The Bramble-Hilbert lemma [12] implies

$$\|\hat{y} - \hat{I}\hat{y}\|_{H^1(\hat{T})} \lesssim \sum_{(i,j) \in \mathcal{S}} \|\partial_{ij}^2 \hat{y}\|_{L^2(\hat{T})},$$

where $\mathcal{S} := \{(1,1), (1,2), (2,1), (2,2)\}$ if \hat{T} is a triangle and $\mathcal{S} := \{(1,1), (2,2)\}$ if \hat{T} is a square. To obtain a similar estimate for $|\hat{y} - \hat{I}\hat{y}|_{H^2(\hat{T})}$, we take advantage of the invariance property $\hat{I}p = p$ for every $p \in \mathbb{P}_1$

$$\|D^2(\hat{y} - \hat{I}\hat{y})\|_{L^2(\hat{T})} \leq \|D^2\hat{y}\|_{L^2(\hat{T})} + \|D^2\hat{I}(p - \hat{y})\|_{L^2(\hat{T})}.$$

Furthermore, concatenating inverse and interpolation estimates together with the Bramble-Hilbert lemma yields

$$\|D^2\hat{I}(p - \hat{y})\|_{L^2(\hat{T})} \lesssim \|\hat{I}(p - \hat{y})\|_{L^2(\hat{T})} \lesssim \|p - \hat{y}\|_{L^\infty(\hat{T})} \lesssim \|D^2\hat{y}\|_{L^2(\hat{T})}.$$

Inserting the three previous estimates into (5.4) and mapping back to T gives

$$\|D^2(y - I_h y)\|_{L^2(T)} \lesssim \|DF_T^{-1}\|_{L^\infty(T)}^2 \|DF_T\|_{L^\infty(\hat{T})}^2 \|y\|_{H^2(T)} \lesssim \|y\|_{H^2(T)},$$

whence

$$\|D_h^2 I_h y\|_{L^2(T)} \lesssim \|y\|_{H^2(T)}.$$

In addition, $\|I_h y\|_{L^2(e)} = 0$ if $e \in \mathcal{E}_h^0$ because $I_h y \in W_\infty^1(\Omega)$ whereas $\|I_h y\|_{L^2(e)} \lesssim h_e^{3/2} \|y\|_{H^2(\omega(e))}$ if $e \in \mathcal{E}_h^b$. Similarly, for all $e \in \mathcal{E}_h^0 \cap \mathcal{E}_h^b$ we have

$$\|\nabla I_h y\|_{L^2(e)} \leq \|\nabla(I_h y^+ - y)\|_{L^2(e)} + \|\nabla(I_h y^- - y)\|_{L^2(e)} \lesssim h_e^{1/2} \|y\|_{H^2(\omega(e))}.$$

Consequently, $E_h[y_h]$ is uniformly bounded and $\|y - y_h\|_{L^2(\Omega)} \lesssim h^2 \|y\|_{H^2(\Omega)}$.

Step 2 (discrete isometry defect). We claim that y_h satisfies (1.6) for $\delta \geq \delta_1$. Since

$$\|\nabla y_h\|_{L^2(T)} \leq \|\nabla y\|_{L^2(T)} + \|\nabla(y_h - y)\|_{L^2(T)} \leq \|\nabla y\|_{L^2(T)} + Ch \|D^2 y\|_{L^2(T)},$$

where C is an interpolation constant that depends on shape regularity of $\{\mathcal{T}_h\}$, adding and subtracting y and recalling that $\nabla y^T \nabla y = I$ a.e. in Ω and $h \leq 1$, we obtain

$$\begin{aligned} D_h[y_h] &\leq \sum_{T \in \mathcal{T}_h} \left(\|\nabla y_h\|_{L^2(T)} + \|\nabla y\|_{L^2(T)} \right) \|\nabla(y - y_h)\|_{L^2(T)} \\ &\lesssim h \sum_{T \in \mathcal{T}_h} \|\nabla y\|_{L^2(T)} \|D^2 y\|_{L^2(T)} + h^2 \sum_{T \in \mathcal{T}_h} \|D^2 y\|_{L^2(T)}^2 \\ &\leq h \|\nabla y\|_{L^2(\Omega)} \|D^2 y\|_{L^2(\Omega)} + h^2 \|D^2 y\|_{L^2(\Omega)}^2 \leq 2\Lambda^2 h. \end{aligned}$$

Therefore, if $\delta_1 = Ch\Lambda^2 = Ch\|y\|_{H^2(\Omega)}^2$, we deduce that $y_h \in \mathbb{A}_{h,\delta}^k$ for $\delta \geq \delta_1$.

Step 3 (convergence of $E_h[y_h]$). It remains to show that as $h, \delta \rightarrow 0$

$$E_h[y_h] \rightarrow E[y].$$

We focus on two critical terms in $E_h[y_h]$ in (2.11), namely

$$\|D_h^2 y_h\|_{L^2(\Omega)} \rightarrow \|D^2 y\|_{L^2(\Omega)}, \quad \|h^{-1/2} [\nabla_h y_h]\|_{L^2(\Gamma_h)} \rightarrow 0,$$

because similar arguments yield $\|h^{-3/2} [y_h]\|_{L^2(\Gamma_h)} \rightarrow 0$ as well as convergence of the remaining terms in $E_h[y_h]$ following Lemma 2.3 (coercivity of E_h).

Since y is merely in $[H^2(\Omega)]^3$, we argue by density. Let $\{y^\varepsilon\}_{\varepsilon>0} \subset [C^\infty(\mathbb{R}^2)]^3$ be a sequence of regularizations of y such that $y^\varepsilon \rightarrow y$ in $[H^2(\Omega)]^3$ as $\varepsilon \rightarrow 0$, and let

$y_h^\varepsilon = I_h^k y^\varepsilon \in [\mathring{\mathbb{V}}_h^k]^3$ be the Lagrange interpolant of y^ε . Exploiting the H^2 -stability of I_h^k , already mentioned in Step 1, leads to

$$\|D_h^2(y_h - y_h^\varepsilon)\|_{L^2(\Omega)} \lesssim \|D^2(y - y^\varepsilon)\|_{L^2(\Omega)},$$

whence writing $y - y_h = (y - y^\varepsilon) + (y^\varepsilon - y_h^\varepsilon) + (y_h^\varepsilon - y_h)$ gives

$$\|D_h^2(y - y_h)\|_{L^2(\Omega)} \lesssim \|y - y^\varepsilon\|_{H^2(\Omega)} + h \|y^\varepsilon\|_{H^3(\Omega)} \rightarrow 0$$

as $h \rightarrow 0$ upon choosing first the coarse scale ε and next h . This implies convergence of norms by the triangle inequality.

We finally examine the stabilization term $\|h^{-1/2} [\nabla_h y_h]\|_{L^2(\Gamma_h)}$. We recall that $[\nabla y] = 0$ for all interior edges $e \in \mathcal{E}_h^0$ and $\nabla y = \Phi$ for boundary edges $e \in \mathcal{E}_h^b$. We next utilize the scaled trace inequality to write

$$\|h^{-1/2} [\nabla_h y_h]\|_{L^2(e)} = \|h^{-1/2} [\nabla_h (y_h - y)]\|_{L^2(e)} \lesssim \|D_h^2(y_h - y)\|_{L^2(\omega(e))},$$

whence $\|h^{-1/2} [\nabla_h y_h]\|_{L^2(\Gamma_h)} \rightarrow 0$ as $h \rightarrow 0$. This concludes the proof. \square

We point out that the uniform bound for $\|D_h^2 y_h\|_{L^2(\Omega)}$ (Step 1) is slightly intricate to account for subdivisions made of quadrilaterals. In fact, in this case the map $F_T : \hat{T} \rightarrow T$ is nonlinear and so (i) mapping to \hat{T} involves all the derivatives up to order 2 and (ii) the Lagrange interpolation operator I_h does not preserve linears. We refer to [18] and [21, Chapter 13] for a detailed discussion of this issue.

5.4. Convergence of global minimizers. We now show that cluster points of global minimizers of E_h are global minimizers of E , without assuming the existence of the latter. The proof combines Lemmas 5.2 (lim-inf property) and 5.3 (lim-sup property) with Lemma 2.3 (coercivity of E_h).

We collect here properties of the *nonconvex* discrete admissible set $\mathbb{A}_{h,\delta}^k$. Given an initial guess $y_h^0 \in \mathbb{V}_h^k$ with isometry defect $D_h[y_h^0] \leq \tau$, the discrete H^2 -gradient flow of Section 3 produces a sequence $\{y_h^n\}_n \subset \mathbb{A}_{h,\delta}^k$ for any $\delta \geq \delta_0$ with

$$\delta_0 = (1 + C_F E_h[y_h^0])\tau,$$

according to Lemma 3.3 (discrete isometry defect). Moreover, Lemma 3.2 (energy decay) guarantees that $\{y_h^n\}_n$ is a Cauchy sequence in the H_h^2 -norm and $E_h[y_h^n] \leq E_h[y_h^0]$ for all $n \geq 1$, whence $y_h = \lim_{n \rightarrow \infty} y_h^n$ is a local minimizer of E_h within $\mathbb{A}_{h,\delta}^k$ and $E_h[y_h] \leq E_h[y_h^0]$. This in turn shows that the set $\mathbb{A}_{h,\delta}^k$ is non-empty provided $\delta \geq \delta_0$ and that if $E_h[y_h^0] \leq \Lambda$, for a constant Λ independent of h , then δ_0 can be made arbitrarily small as $\tau \rightarrow 0$. We could take τ proportional to h , which is the choice in Section 6.

Theorem 5.4 (convergence of global minimizers). *Let data (g, Φ, f) satisfy (1.2) and set*

$$\Lambda_0 := \|g\|_{H^1(\Omega)}^2 + \|\Phi\|_{H^1(\Omega)}^2 + \|f\|_{L^2(\Omega)}^2.$$

Let the penalty parameters γ_0 and γ_1 in (2.11) be chosen sufficiently large. Let $y_h \in \mathbb{V}_h^k(g, \Phi)$ be a sequence of functions such that $E_h[y_h] \leq \Lambda_1$ for a constant Λ_1 independent of h . Let the discrete isometry defect parameter δ satisfy

$$\delta \geq \delta_1 := C(\Lambda_0 + \Lambda_1)h,$$

where C is an interpolation constant depending on the shape regularity of $\{\mathcal{T}_h\}$. If $y_h \in \mathbb{A}_{h,\delta}^k$ is an almost global minimizer of E_h , namely

$$E_h[y_h] \leq \inf_{w_h \in \mathbb{A}_{h,\delta}} E_h[w_h] + \epsilon,$$

where $\epsilon, \delta \rightarrow 0$ as $h \rightarrow 0$, then $\{y_h\}_h$ is precompact in $[L^2(\Omega)]^3$ and every cluster point y of y_h belongs to \mathbb{A} and is a global minimizer of E , namely $E[y] = \inf_{w \in \mathbb{A}} E[w]$. Moreover, up to a subsequence (not relabeled), the energies converge

$$\lim_{h \rightarrow 0} E_h[y_h] = E[y].$$

Proof. This proof is standard and given for completeness. Since $E_h[y_h] \leq \Lambda_1$, we invoke Lemma 5.2 (lim-inf property) to deduce the existence of $y \in \mathbb{A}$ such that (a non-relabeled subsequence) $y_h \rightarrow y$ in $[L^2(\Omega)]^3$ and

$$E[y] \leq \liminf_{h \rightarrow 0} E_h[y_h].$$

This means that \mathbb{A} is non-empty and that

$$\inf_{z \in \mathbb{A}} E[z] \leq E[y] \leq \Lambda_1.$$

To show that y is a global minimizer of E , we let $0 < \eta < 1$ and $w \in \mathbb{A}$ satisfy

$$E[w] \leq \inf_{z \in \mathbb{A}} E[z] + \eta.$$

Using Lemma 2.2 (coercivity of E), we deduce that $\|w\|_{H^2(\Omega)}^2 \lesssim \Lambda_0 + \Lambda_1$, which enables us to resort to Lemma 5.3 (lim-sup property) with $\delta \geq \delta_1$ to exhibit a recovery sequence $w_h \in \mathbb{A}_{h,\delta}^k$ of w such that $w_h \rightarrow w$ in $[L^2(\Omega)]^3$ as $h, \delta \rightarrow 0$ and

$$\limsup_{h, \delta \rightarrow 0} E_h[w_h] \leq E[w].$$

We next utilize that $E_h[y_h] \leq E_h[w_h] + \epsilon$, because y_h is an almost global minimizer of E_h within $\mathbb{A}_{h,\delta}^k$ and $w_h \in \mathbb{A}_{h,\delta}^k$, to derive

$$E[y] \leq \liminf_{h \rightarrow 0} E_h[y_h] \leq \limsup_{h \rightarrow 0} (E_h[w_h] + \epsilon) \leq E[w] \leq \inf_{z \in \mathbb{A}} E[z] + \eta.$$

Taking $\eta \rightarrow 0$ implies that y is an global minimizer of E and

$$\lim_{h \rightarrow 0} E_h[y_h] = E[y].$$

This concludes the proof. \square

5.5. Strong Convergence of $H_h[y_h]$ and Scaled Jumps. We now exploit Theorem 5.4 (convergence of global minimizers) to strengthen the results of Proposition 5.1 (compactness in $L^2(\Omega)$), in the spirit of [19, 30]. In fact, we show strong convergence of the scaled jump terms to zero and of the discrete Hessian $H_h[y_h]$ of y_h to D^2y as $h \rightarrow 0$.

Corollary 5.1 (strong convergence of Hessian and scaled jumps). *Let (g, Φ, f) satisfy (1.2) and the penalty parameters γ_0 and γ_1 in (2.11) be chosen sufficiently large. Let $y_h \in \mathbb{A}_{h,\delta}^k$ be a sub-sequence of almost global minimizers of E_h converging to a global minimizer $y \in \mathbb{A}$ of E , as established in Theorem 5.4 (convergence of global minimizers). Then, the following statements are valid as $h \rightarrow 0$*

- (i) $H_h[y_h] \rightarrow D^2y$ strongly in $[L^2(\Omega)]^{3 \times 2 \times 2}$;
- (ii) $\|h^{-1/2}[\nabla_h y_h]\|_{L^2(\Gamma_h)} + \|h^{-3/2}[y_h]\|_{L^2(\Gamma_h)} \rightarrow 0$;
- (iii) $D_h^2 y_h \rightarrow D^2y$ strongly in $[L^2(\Omega)]^{3 \times 2 \times 2}$.

Proof. We first observe that Theorem 5.4 (convergence of global minimizers) yields

$$E_h[y_h] \rightarrow E[y] = \frac{1}{2} \int_{\Omega} |D^2 y|^2 - \int_{\Omega} f y, \quad \text{as } h \rightarrow 0.$$

We apply Proposition 4.4 (relation between $E_h[y_h]$ and H_h) to deduce

$$\frac{1}{2} \limsup_{h \rightarrow 0} \|H_h[y_h]\|_{L^2(\Omega)}^2 \leq \limsup_{h \rightarrow 0} \left(E_h[y_h] + \int_{\Omega} f y_h \right) = \frac{1}{2} \|D^2 y\|_{L^2(\Omega)}^2.$$

Combining Proposition 4.3 (weak convergence of $H_h[y_h]$), namely $H_h[y_h] \rightharpoonup D^2 y$ in $L^2(\Omega)$, with the lower semi-continuity of the L^2 -norm, we obtain

$$\|D^2 y\|_{L^2(\Omega)}^2 \leq \liminf_{h \rightarrow 0} \|H_h[y_h]\|_{L^2(\Omega)}^2,$$

whence

$$\|H_h[y_h]\|_{L^2(\Omega)} \rightarrow \|D^2 y\|_{L^2(\Omega)}.$$

Weak convergence and convergence of norms imply strong convergence, and so (i).

To prove (ii) we make use of (i) to infer that as $h \rightarrow 0$

$$E_h[y_h] - \frac{1}{2} \int_{\Omega} |H_h[y_h]|^2 + \int_{\Omega} f y_h \rightarrow E[y] - \frac{1}{2} \int_{\Omega} |D^2 y|^2 + \int_{\Omega} f y = 0.$$

We now take advantage of the representation (4.9) to find that $I_h \rightarrow 0$ as $h \rightarrow 0$ and, in view of (4.10), that

$$\|h^{-3/2}[y_h]\|_{L^2(\Gamma_h)} + \|h^{-1/2}[\nabla_h y_h]\|_{L^2(\Gamma_h)}^2 \rightarrow 0 \quad \text{as } h \rightarrow 0.$$

This not only establishes (ii), but combined with (i) and the definition (4.7) of $H_h[y_h]$ and the bounds (4.8) for R_h and B_h , directly implies (iii). \square

6. NUMERICAL EXPERIMENTS

In this section we explore and compare the performance of our method with that of the Kirchhoff elements. We are interested in the speed and accuracy of the method, as well as its ability to capture the physics and the geometry of the problems appropriately. We observe that our dG approach seems to be more flexible with comparable or better speed. We present specific examples in the rest of this section computed within the platform deal.ii with polynomial degree $k = 2$ [1, 4]; hence we use $\mathbb{Q}_2(T)$ for all $T \in \mathcal{T}_h$. Moreover, one might notice that we consistently use rather large penalty parameters γ_0, γ_1 relative to the second-order case. These choices hinge mostly on experiments performed for the vertical load example of Subsection 6.1 and are not dictated by stability considerations exclusively. In fact, they are a compromise between the discrete initial energy $E_h[y_h^0]$ and the fictitious time step τ of the gradient flow, which obey the relations (3.7) and (3.8) and control the discrete isometry defect $D_h[y_h]$ according to (3.9). We point out that enforcing Dirichlet conditions via the Nitsche's approach depends on γ_0 and γ_1 and affects $E_h[y_h^0]$. We examined a very wide range of γ_0 and γ_1 and compared $D_h[y_h]$ and the rate at which it decreases for each tested pair. We selected those values that lead to the smallest defect and the largest rate of convergence. We made similar choices for all subsequent examples without exhaustive testing for each of them. We note that our theory does not explicitly predict why the best convergence behavior manifests for such large values of γ_0 and γ_1 . We do not provide our computational study leading to γ_0 and γ_1 , for the sake of brevity.

6.1. Vertical load on a square domain. This is a simple example of bending due to vertical load. We use the same configuration as in [5] in order to provide an accurate comparison of the two methods. We deal with a square domain with two of the non-parallel sides being clamped.

Example 6.1. Let $\Omega = (0, 4) \times (0, 4)$ and $\partial_D \Omega = \{0\} \times [0, 4] \cup [0, 4] \times \{0\}$ be the part of the boundary where we enforce the boundary conditions

$$g = (x_1, x_2, 0) \quad \text{and} \quad \Phi = [I_2, 0]^T.$$

We apply a vertical force of magnitude 2.5×10^{-2} .

We first illustrate the convergence of the energy $E_h[y_h]$ and the isometry defect $D_h[y_h]$ as the mesh size decreases. We set $\gamma_0 = 5,000$, $\gamma_1 = 1100$ and choose $\tau = h$ and observe that the isometry defect decays super-linearly with τ , which is better than the linear convergence predicted in Lemma 3.3 (discrete isometry constraint). Compared to [5], we obtain a more clear rate, while the defect itself is smaller, up to one order of magnitude. The number of gradient flow iterations is similar for both methods.

No. Cells	DoFs	$\tau = h$	$E_h[y_h]$	$D_h[y_h]$	Iterations
256	7680	$\sqrt{2} \ 2^{-2}$	-7.53e-3	4.02e-3	13
1024	30,720	$\sqrt{2} \ 2^{-3}$	-5.76e-3	1.63e-3	28
4096	122,880	$\sqrt{2} \ 2^{-4}$	-4.26e-3	6.07e-4	76
16384	491,520	$\sqrt{2} \ 2^{-5}$	-3.30e-3	2.28e-4	140

TABLE 1. Number of cells, degrees of freedom, discrete energy $E_h[y_h]$, isometry defect $D_h[y_h]$ and number of gradient flow iterations for square plate, clamped in two sides with vertical forcing. We observe super-linear rates for the isometry defect, while theory predicts linear rates for the case $\tau = h$.

We now explore the geometric behavior of our method. More precisely, it was observed in [5] that there was an artificial displacement along the diagonal $x_1 + x_2 = 4$, which does not correspond to the actual physics of the problem, $y = 0$ for $x_1 + x_2 \leq 4$. This displacement decreases with smaller mesh size. Our method introduces the same artificial deformation. However, we can see in the following figure that i./n our case this displacement is smaller, even by one order of magnitude for the last refinement.

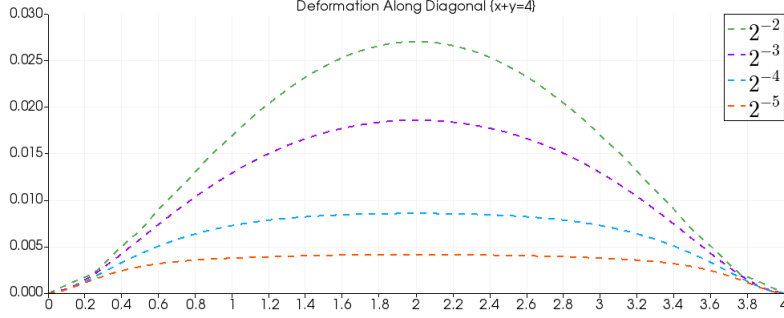


FIGURE 1. Deformation along the diagonal $x_1 + x_2 = 4$. We observe smaller deformation y than with the Kirchhoff elements, up to one order of magnitude. For example, $h = 2^{-3}$ yields $|y| \approx 0.018$ for dG, while $h = 2^{-6}$ gives $|y| \approx 0.02$ for Kirchhoff elements.

6.2. Obstacle Problem. In the previous example we observe some of the flexibility of the dG approach in terms of capturing the physical behavior of the plates. To explore this further, we introduce an extra element to the deformation: an obstacle. We use a square plate clamped on one side and we exert a vertical force. We require that the plate does not penetrate the obstacle. We choose a simple case where the obstacle is a rigid flat plate at height $z = 0.2$. This example is motivated by [7], where the deformation of the plate is the result of thermal actuation of bilayer hinges connected to the plate. In our case, we use a vertical load instead. From a mathematical viewpoint, this obstacle problem can be treated by introducing the convex set of the constraint

$$K = \{y \in [L^2(\Omega)]^3 \mid y_3 \leq 0.2\},$$

along with a splitting of variables. We introduce another deformation s , $s \approx y$ such that $s \in K$ always and penalize the $L^2(\Omega)$ -distance between y and s . If ε is an obstacle penalty parameter, we add the following extra term to the energy $E[y]$

$$\frac{1}{\varepsilon} \|y - s\|_{L^2(\Omega)}^2.$$

At the discrete level, this affects the gradient flow at each step, where we use as s_h the L^2 -projection of the previous solution y_h^n in K . We refer to [7] for more details about the variable splitting and the projection.

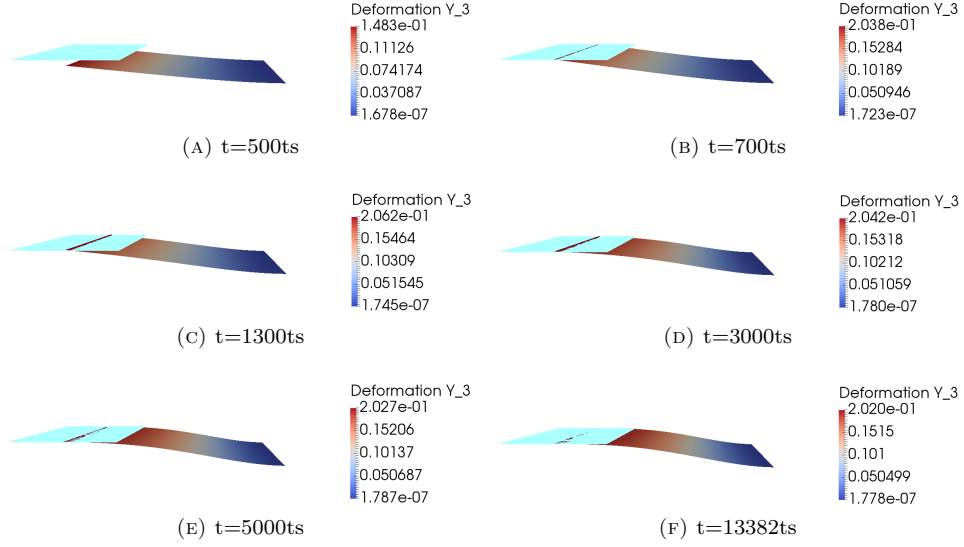


FIGURE 2. Deformation of the plate: (a) Initial stage, deformation determined only by forcing, (b) First contact with the obstacle, (c) Penetration of the obstacle, (d) Starts adjusting shape to decrease crossing, (e) Stronger bending, decreased crossing, (f) Final stage, crosses obstacle by 0.002.

Example 6.2. Let $\Omega = (-1, 1) \times (-1, 1)$. Let $\partial_D \Omega = \{-1\} \times [-1, 1]$ be the part of the boundary where we enforce clamped boundary conditions. We apply a vertical force $f = (0, 0, 1)$.

To describe the performance of our method, we first present the deformation of the plate for three different time steps for the same configuration but without any obstacle. The plate remains clamped on the side while the third component increases and the plate eventually bends. From a physical viewpoint we would expect that the obstacle would make no difference at the first steps of the deformation. However, when the plate meets the obstacle, we expect it to stop rising and start bending accordingly so that it complies with the obstacle and the force. This is indeed the case. The plate rises until it meets the obstacle and then adjusts by bending. However, since we do not force y_h numerically to belong to the set K , but rather penalize its L^2 -distance from its projection in K , we see that there is a minor penetration of the obstacle. The plate adjusts to the presence of the obstacle and this crossing decreases. This behavior can be enhanced by further refining and by choosing the obstacle parameter ε to be smaller. We set $\gamma_0 = \gamma_1 = 5000$. To illustrate the deformation, we provide six different steps of the flow in Figure 2. The illustration corresponds to 1024 cells, $\varepsilon = 3 \times 10^{-4}$ and time step $\tau = 5 \times 10^{-4}$. The isometry defect at the end of this simulation is only 9×10^{-5} .

6.3. Compressive Case. As our last example, we explore another geometrically and physically interesting case, that of buckling. We use a rectangular plate with a small vertical load and we impose compressive boundary conditions at two opposite sides. This example is also motivated by [5].

Example 6.3. Let $\Omega = (-2, 2) \times (0, 1)$. Let also $\partial_D \Omega = \{-2, 2\} \times [0, 1]$ be the two sides where we impose the compressive boundary conditions

$$g = (x_1 \pm 1.4, x_2, 0) \quad \text{and} \quad \Phi = [I_2, 0]^T.$$

We apply a vertical force f of magnitude 10^{-2} . Given the compressive nature of the problem, the plate could bend either upwards or downwards (buckling), resulting in two deformations which are the reflection of each other with respect to the $x_1 - x_2$ plane and have the same minimizing energy. This is why we apply a small force, in order to select one of the two deformations, which in our case corresponds to a positive third component. We note here that we need a stronger force than the one in [5] (10^{-5}). Since we start again with a flat configuration as our initial guess y_h^0 , the Nitsche boundary terms yield a large initial energy $E_h[y_h^0]$. This possibly explains why we may require a stronger force than in [5] in order to guide this energy towards one or the other minimizing states. Moreover, in order to prevent the large initial energy from creating a very abrupt and non-physical deformation in the gradient flow, we employ an approach of quasi-static nature: we do not enforce the boundary conditions from the beginning of the flow, but rather do it gradually (parameter continuation). We use a parameter α that starts from zero and increases throughout the flow until it reaches the value 1. In order to achieve a gradual adjustment to the boundary conditions, we let

$$\varphi(\alpha) := (1 - \alpha) \, id + \alpha \, g, \quad 0 \leq \alpha \leq 1,$$

and $\Phi(\alpha) = \Phi$ be the Dirichlet boundary conditions for y and ∇y , where id stands for the identity function. As the mesh becomes finer, parameter α needs to grow slower, in order to compensate for the big initial energy and allow for a more natural flow. To illustrate the effect of α , we depict in Figure 3 the deformation that corresponds to various stages of the gradient flow with $\gamma_0 = \gamma_1 = 10000$ and time step $\tau = 0.04625$. The parameter α increases linearly by 5×10^{-5} in each iteration. We see that the compressive nature of the boundary conditions becomes more apparent after α becomes greater than $1/2$ and that the boundary conditions are achieved at the end of the deformation. The final isometry defect is $D_h[y_h] = 5.04 \cdot 10^{-3}$, one order of magnitude smaller than observed in [5].

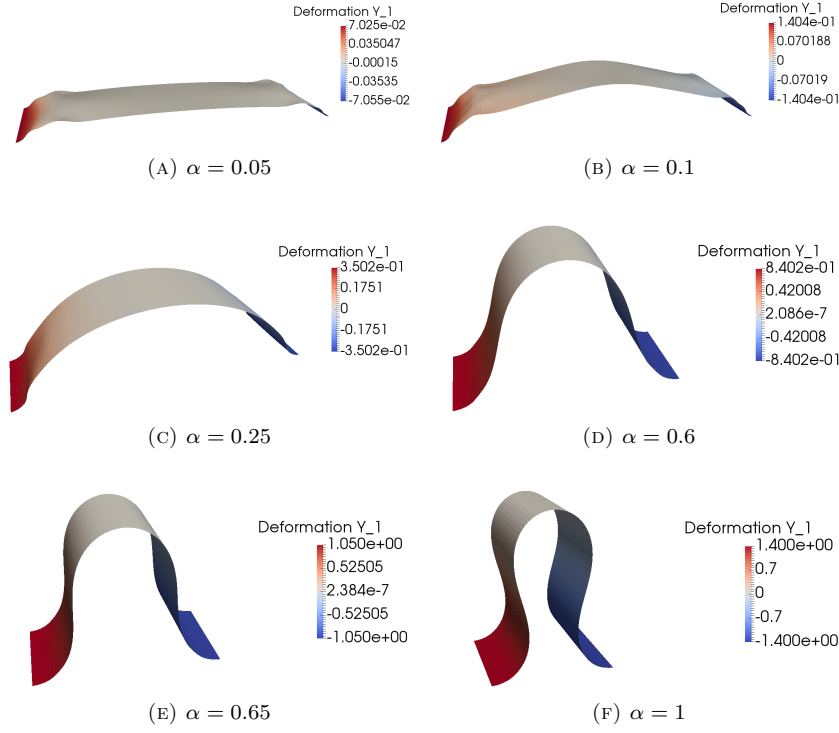


FIGURE 3. Deformation of the plate at six different stages: (a)-(c) Initial stages, slow deformation determined mostly by the forcing, (d)-(e) The compressive boundary conditions become more active and determine the shape of the plate, (f) Final deformation, compressive boundary conditions are achieved.

7. IMPLEMENTATION

Before we conclude, we wish to make some implementation remarks and connect them with the theory in Section 2 and Section 3. We see in Section 3 that we solve (3.4) for $\delta y_h^{n+1} \in \mathcal{F}_h^n[y_h^n]$. In order to implement the linearized isometry constraint (3.2), we search for $\delta y_h^{n+1} \in \mathbb{V}_h^2$ and a *symmetric* piecewise constant Lagrange multiplier $\lambda_h^{n+1} \in [\mathbb{V}_h^0]^{2 \times 2}$ such that (3.4) is satisfied and

$$(7.1) \quad \int_T \lambda_h^{n+1} : ((\nabla \delta y_h^{n+1})^T \nabla y_h^n + (\nabla y_h^n)^T \nabla \delta y_h^{n+1}) = 0 \quad \forall T \in \mathcal{T}_h.$$

This creates a saddle-point problem formulation and a linear system of the form

$$(7.2) \quad \begin{bmatrix} A & B_n^T \\ B_n & 0 \end{bmatrix} \begin{bmatrix} \delta Y_h^{n+1} \\ \Lambda_h^{n+1} \end{bmatrix} = \begin{bmatrix} F_n \\ 0 \end{bmatrix},$$

where A is the matrix corresponding to the first two terms of (3.4) that involve the coercive bilinear form a_h and the discrete inner product $(\cdot, \cdot)_{H_h^2}$, B_n^T is the matrix that corresponds to (7.1) and depends on y_h^n and the bold symbols correspond to the vectorized forms of δy_h^{n+1} , λ_h^{n+1} and the right-hand side of (3.4). Since A does

not depend on y_h^n we can assemble it and obtain its LU decomposition once and subsequently use a direct solver whenever we need to use A^{-1} . For the full system we use the Schur complement with a conjugate gradient iterative solver, in order to solve for Λ_h^{n+1} and then recover δY_h^{n+1} . Although it is not clear, at this point, whether an inf-sup condition for the saddle point problem is valid and yields a pair $(\lambda_h^{n+1}, \delta y_h^{n+1})$ with a non-zero δy_h^{n+1} , our numerical experiments in Section 6 reveal that such a pair exists and leads to small isometry defects at the end of the flow. Lastly, it is important to mention that our choice of a discontinuous space \mathbb{V}_h^k in Section 2 is strongly motivated by the implementation of (7.1) and (7.2). To be more precise, choosing continuous functions in \mathbb{V}_h^k would make (7.1) harder to achieve, because an element-wise satisfaction of (7.1) would also need to respect the continuity of δy_h^{n+1} . In fact, computational experiments for continuous functions (not reported here) indicate that the conjugate gradient method becomes significantly slower if the functions of \mathbb{V}_h^k are required to be continuous; this explains our choice of a fully discontinuous space \mathbb{V}_h^k . We refer to [28] for details.

8. CONCLUSIONS

In this work we design and implement a dG approach to construct minimizers for large bending deformations under a non-linear isometry constraint. We derive a discrete energy functional and provide a flexible approximation of the isometry constraint. We employ a discrete approximation of the Hessian inspired by [19] and [30] to prove the Γ -convergence of the discrete energy to the continuous one and combine it with a compactness argument to prove that global minimizers of the discrete energy converge in L^2 to global minimizers of the continuous energy. The existence of the latter is not assumed a-priori, but is rather a consequence of our analysis. Our dG approach simplifies some implementation details and theoretical constructions needed in [5] for the Kirchhoff elements. Moreover, we present numerical experiments that indicate that the dG approach also captures the physics of some problems better than the Kirchhoff approach, while also giving rise to a more accurate approximation of the isometry constraint.

REFERENCES

1. D. Arndt, W. Bangerth, D. Davydov, T. Heister, L. Heltai, M. Kronbichler, M. Maier, J.-P. Pelteret, B. Turcksin, D. Wells, *The deal.II Library, Version 8.5*, Journal of Numerical Mathematics, 25(3):137–146, 2017.
2. D. N. Arnold, F. Brezzi, B. Cockburn, L. D. Marini, *Unified Analysis of Discontinuous Galerkin Methods for Elliptic Problems*, SIAM J. Numer. Anal., 39(5), 1749–1779, 2002.
3. E. Bänsch, P. Morin, R.H. Nochetto, *An adaptive Uzawa FEM for the Stokes problem: Convergence without the inf-sup condition*, SIAM J. Numer. Anal. 40 (2002), 1207–1229.
4. W. Bangerth, R. Hartmann, G. Kanschat, *deal.II – a General Purpose Object Oriented Finite Element Library*, ACM Trans. Math. Softw., 33(4):24/1–24/27, 2017.
5. S. Bartels, *Finite element approximation of large bending isometries*, Numer. Math. 124, 3, 415–440, 2013.
6. S. Bartels, *Numerical Methods for Nonlinear Partial Differential Equations*, Springer International Publishing, 2015.
7. S. Bartels, A. Bonito, Anastasia H. Muliana, R. H. Nochetto, *Modeling and simulation of thermally actuated bilayer plates*, arXiv:1704.01849, 2017.
8. S. Bartels, A. Bonito, R. H. Nochetto, *Bilayer Plates: Model Reduction, Γ -Convergent Finite Element Approximation and Discrete Gradient Flow*, Commun. Pure Appl. Math., 2015.
9. N. Bassik, B. Abebe, K. Laffin, D. Gracias, *Photolithographically patterned smart hydrogel based bilayer actuators*, Polymer 51, 6093–6098, 2010.

10. K. Bhattacharya, M. Lewicka, M. Schaffner, *Plates with incompatible prestrain*, arXiv:1401.1609, 2014.
11. A. Bonito, R. H. Nochetto, *Quasi-Optimal Convergence Rate of an Adaptive Discontinuous Galerkin Method*, SIAM J. Numer. Anal., 48(2), 734-771, 2010.
12. J.H. Bramble, S.R. Hilbert, *Bounds for a class of linear functionals with applications to Hermite interpolation*, Numer. Math., 16, 362-369, 1970/71.
13. S. C. Brenner, *Poincaré-Friedrichs Inequalities for Piecewise H^1 Functions*, SIAM J. Numer. Anal., 41(1), 306-324, 2003.
14. S. C. Brenner, *Two-level additive Schwarz preconditioners for nonconforming finite elements*, Math. Comp., 65(215), 897-921, 1996.
15. S. C. Brenner, K. Wang, J. Zhao, *Poincaré-Friedrichs Inequalities for Piecewise H^2 Functions*, Numer. Funct. Anal. Optim., 25, 463-478, 2004.
16. F. Brezzi, G. Manzini, D. Marini, P. Pietra, A. Russo, *Discontinuous Galerkin approximations for elliptic problems*, Numer. Methods Partial Differential Equations, 16(4), 365-378, 2000.
17. A. Buffa, C. Ortner, *Compact embeddings of broken Sobolev spaces and applications*, IMA Numer. Anal., 29, 827-855, 2009.
18. P.G. Ciarlet, P.-A. Raviart, *Interpolation theory over curved elements, with applications to finite element methods*, Comput. Methods Appl. Mech. Engrg., 1, 217-249, 1972.
19. D. A. Di Pietro, A. Ern, *Discrete Functional Analysis Tools for Discontinuous Galerkin Methods with Application to the Incompressible Navier-Stokes Equations*, Math. Comp., 79(271), 1303-1330, 2010.
20. A. Ern, J-L Guermond, *Finite element quasi-interpolation and best approximation*, ESAIM: M2AN 51, 1367-1385, 2017.
21. A. Ern, J-L Guermond, *Finite Elements I: Approximation and interpolation*, to appear.
22. G. Friesecke, R.D. James, S. Müller *A theorem on geometric rigidity and the derivation of nonlinear plate theory from three-dimensional elasticity*, Comm. Pure Appl. Math. 55, 11, 1461-1506, 2002.
23. E. Jager, E. Smela, O. Inganäs, *Microfabricating conjugated polymer actuators*, Science 290, 1540-1545, 2000.
24. R.H.W. Hoppe, B. Wohlmuth, *Element-oriented and edge-oriented local error estimators for nonconforming finite element methods*, RAIRO Modél. Math. Anal. Numér., 30(2), 237-263, 1996.
25. P. Hornung, *Approximation of flat $W^{2,2}$ isometric immersions by smooth ones*, Arch. Ration. Mech. Anal. 199, 1015- 1067, 2011.
26. J.-N. Kuo, G.-B. Lee, W.-F. Pan, H.-L. Lee, *Shape and thermal effects of metal films on stress-induced bending of micromachined bilayer cantilever*, Japanese Journal of Applied Physics 44, 5R, 3180, 2005.
27. M. Lewicka, P. Ochoa, M.-R. Pakzad, *Variational models for prestrained plates with Monge-Ampère constraint*, Differential Integral Equations 28, no. 9/10, 861-898, 2015.
28. D. Ntoggas, *Non-linear geometric PDEs: algorithms, numerical analysis and computation*, PhD Thesis, University of Maryland, College Park, 2018.
29. P. Oswald, *On a BPX-preconditioner for P1 elements*, Computing, 51(2), 125-133, 1993.
30. T. Pryer, *Discontinuous Galerkin methods for the p -biharmonic equation from a discrete variational perspective*, Electronic Transactions of Numerical Analysis, 2014.
31. B. Rivière, *Discontinuous Galerkin methods for solving elliptic and parabolic equations: theory and implementation*, Society for Industrial and Applied Mathematics, 2008.
32. O. Schmidt, K. Eberl, *Thin solid films roll up into nanotubes*, Nature 410, 168, 2001.
33. E. Smela, O. Inganäs, I. Lundström, *Controlled folding of micrometer-size structures*, Science 268, 5218, 17351738, 1995.

DEPARTMENT OF MATHEMATICS, TEXAS A&M UNIVERSITY, COLLEGE STATION, TX 77843
E-mail address: bonito@math.tamu.edu

DEPARTMENT OF MATHEMATICS AND INSTITUTE FOR PHYSICAL SCIENCE AND TECHNOLOGY,
 UNIVERSITY OF MARYLAND, COLLEGE PARK, MARYLAND 20742
E-mail address: rhn@math.umd.edu

DEPARTMENT OF MATHEMATICS, UNIVERSITY OF MARYLAND, COLLEGE PARK, MARYLAND 20742
E-mail address: dimnt@math.umd.edu